



OPEN Effects of whole brain proton irradiation at conventional or ultra-high dose rate (FLASH), in adult male Sprague Dawley rats

Michael T. Williams^{1,2,3✉}, Samantha L. Regan^{1,2,6}, Adam L. Fritz², Brooke M. Gollaway², Anthony E. Mascia^{1,3,4,5}, Ralph E. Vatner^{3,4}, John P. Perentesis^{1,3,5} & Charles V. Vorhees^{1,2,3}

Radiation is an effective treatment for many brain tumors, but often causes cognitive impairment. Ultra-high dose rate (FLASH) radiotherapy is less toxic to many normal tissues and may protect against adverse cognitive effects of cranial irradiation. Adult male Sprague Dawley rats received a single 18 Gy fraction of cranial irradiation with protons at 1 Gy/s (CV), 60 Gy/s (FLASH-60), 95 Gy/s (FLASH-95), or sham treatment (Control) ($n \geq 22/\text{group}$). Rats were tested in open-field, acoustic (ASR) and tactile startle (TSR), novelty preference, radial water maze (RWM), Morris water maze (MWM), Cincinnati water maze configurations A and B (CWM-A CWM-B), and novelty tests. Locomotion was decreased and TSR increased in all irradiated rats and ASR increased in FLASH-95 rats compared with Controls. In MWM acquisition and reversal, the CV and FLASH-60 rats had reduced path efficiency but during shift and shift reversal all irradiated rats had increased latencies and reduced path efficiencies compared with Controls. In CWM-A all irradiated rats performed below Controls. There were no differences found in CWM-B, novelty tests, or RWM. In summary, FLASH treatment after 18 Gy cranial proton irradiation did not result in reduced cognitive toxicity.

Keywords Cognition, Spatial learning and memory, Egocentric learning, Memory, Working memory, Proton radiotherapy, FLASH effect

Radiation therapy is an important treatment for reducing the morbidity and mortality associated with both primary and metastatic brain tumors; however, this treatment can affect the adjacent normal brain tissue causing long-term cognitive deficits¹. For this reason, focal irradiation of tumors utilizing advanced radiation techniques (e.g. intensity modulated X-ray therapy, stereotactic radiosurgery, and proton therapy) is performed whenever possible with the goal of minimizing radiation exposure to adjacent normal brain tissue, especially radiosensitive brain regions such as the hippocampus². Compared with photon (X-ray) therapy, proton therapy can further reduce exposure of normal brain tissue when delivering focal treatments but does not completely alleviate later cognitive impairments³. Unfortunately, there are situations where it is necessary to target and treat the whole brain with no possibility of sparing normal brain tissue and the associated cognitive toxicities even with advanced techniques. Adult patients experience measurable cognitive impairments from whole brain irradiation, but these impairments are even more severe for pediatric patients due to the sensitivity of the developing brain to ionizing radiation.

Rodent models of toxicities resulting from cranial irradiation replicate the clinical findings, with juvenile rats experiencing equivalent deficits in a 5-choice serial reaction test after a single fraction of cranial irradiation with X-rays (10 Gy) or a biologically equivalent dose of spread out Bragg peak protons (9.1 Gy) compared with sham treated controls⁴. Differences in MRI imaging characteristics of the brain were identified between photon and

¹Department of Pediatrics, University of Cincinnati College of Medicine, Cincinnati, OH 45229, USA. ²Division of Neurology (MLC 7044), Cincinnati Children's Hospital Medical Center, 3333 Burnet Ave, Cincinnati, OH 45229-3039, USA. ³Cincinnati Children's/University of Cincinnati Proton Therapy and Research Center, Cincinnati, OH 45229, USA. ⁴Department of Radiation Oncology, University of Cincinnati College of Medicine, Cincinnati, OH 45267, USA. ⁵Division of Oncology, Cincinnati Children's Hospital Medical Center, Cincinnati, OH 45229, USA. ⁶Present address: Department of Human Genetics, University of Michigan Medical Center, 3703 E. Catherine St., Ann Arbor, MI 48109-5618, USA. ✉email: michael.williams@cchmc.org

proton treated rats, suggesting some differences in the radiobiology between the two modalities despite similar cognitive toxicity. Adult rats treated with cranial irradiation with protons at doses of 11–17 Gy induced deficits in several cognitive domains that included egocentric and allocentric learning and memory, working memory, as well as impairments in other behaviors, reproducing the toxicity experienced by patients treated with similar or higher doses of fractionated whole brain irradiation with photons or protons, and demonstrating the need for novel approaches for sparing cognitive function, even with proton radiotherapy⁵. Emerging data suggest that radiotherapy delivered at ultra-high dose rates (FLASH) may result in reduced normal tissue toxicity with equivalent tumor control, known as the FLASH effect, and this is one potential approach for greater protection against cranial irradiation induced cognitive toxicity^{6–9}.

Most studies demonstrating the FLASH effect have utilized high energy electron beams, with normal tissue protection seen in zebrafish, mice, minipigs, and cats^{10–14}. In one early study of mice treated with 10 Gy whole brain irradiation with electrons at dose rates that ranged from 0.1 (conventional dose rate) to 500 Gy/s, novelty preference was preserved two months after exposure at dose rates above 60 Gy/s¹⁵. Novel object recognition (NOR) was spared after 10 or 12 Gy cranial irradiation with electrons at a FLASH dose rate compared with mice treated to the same doses at a lower conventional dose rate, and this relative sparing was lost at 14 Gy. Other behavioral tests showed relative sparing with 10 Gy electron FLASH on tests of temporal order, light–dark preference, forced swim, and extinction after conditioned freezing¹². Similar findings were observed in mice with brain tumors treated with a single 10 or 14 Gy fraction of whole brain electron irradiation, with sparing of novelty preference after 10 Gy FLASH treatment (a range of rates were used but all were over 100 Gy/s) compared with the same 10 Gy dose at a conventional dose rate (0.1 Gy/s), but deficits were observed at 14 Gy regardless of dose rate¹⁶. Interestingly, sparing of NOR and novel place recognition was found after 30 Gy whole brain irradiation with electrons at FLASH dose rates compared with the same treatment at a lower conventional dose rate. This sparing of novelty preference differences with FLASH treatment was also observed when delivered in two fractions of 7 Gy, but sparing with FLASH was lost when the treatment was further fractionated into four treatments of 3.5 Gy¹⁶. Three week old mice treated with whole brain irradiation in two 10 Gy fractions of electrons delivered at conventional (0.09 Gy/s) or FLASH dose rates (5.6×10^6 Gy/s) resulted in relative sparing of novel location preference (an object is moved to a new location where an object had not been previously) and NOR with FLASH, but no sparing was observed with FLASH versus conventional dose rate treatment in the light dark test or in social interactions of females¹⁷. While these studies are informative, electron beams do not have the penetrating power to be useful in the clinic for brain radiotherapy in patients.

Studies of the FLASH effect using proton beams have been performed in humans, rats, and mice^{9,18–23}. In regard to cognitive effects, relative sparing of egocentric learning and memory was reported in postnatal day (P)11 rats treated with 5 Gy whole brain irradiation with protons at FLASH (100 Gy/s) and conventional (1 Gy/s) dose rates, when tested as adults¹⁹. No sparing was observed in P11 rats treated with 8 Gy proton FLASH. In a different study, adult rats given 25 Gy whole brain irradiation at a conventional dose rate (4 Gy/s) or FLASH (257 Gy/s) did not exhibit any relative protection on behavioral outcomes in an open field or home-cage wheel running test²⁰. While novelty was tested in the latter study, there was no significant difference in this test among the conventional, FLASH, and sham treated controls however, the small number of subjects tested may have compromised the statistical power, making the results difficult to interpret. These published reports are intriguing and suggest that whole brain irradiation delivered at FLASH dose rates may cause less neurocognitive toxicity compared with the same treatment delivered at conventional dose rates, motivating the need for further investigation of the potential sparing of cognitive deficits following whole brain irradiation with protons delivered at FLASH versus conventional dose rates, utilizing a range of tests of multiple cognitive and behavioral domains.

In this study, adult male Sprague Dawley rats (P66 at treatment) were used to evaluate the effect of 18 Gy cranial irradiation with protons delivered at a conventional dose rate of 1 Gy/s (CV) or FLASH dose rates of 60 Gy/s (FLASH-60) or 95 Gy/s (FLASH-95), with sham treated controls for comparison (Sham: anesthetized with isoflurane and placed under the beam nozzle but not irradiated). The 18 Gy dose was selected for several reasons (1) to ensure that cognitive deficits would develop in these rats as we saw with other doses⁵, (2) our previous study did not use a collimator, the dose response was flat, and a higher dose seemed warranted, and (3) the majority of FLASH data in mice showed electron irradiation induced deficits in novelty recognition, although in rats at a dose of 17 Gy novelty was unaffected and therefore a higher dose was used. This last point was important since it suggested that rats are affected differently than mice and this might apply to the FLASH effect as well. Therefore, while the novel object effect fades away following 14 Gy in mice, there are no data showing that this is true for all species or that it was true for other cognitive realms. Behavioral tests were used to examine different brain structures and functions, with multiple structures involved in the types of learning and memory assessed. Using a test battery reduces the number of rats needed to characterize different cognitive and behavioral domains and is more comparable to human outcome tests^{24,25}. Tests were run from least to most stressful²⁶. Rats were assessed at 5 times post-irradiation for open-field activity (bi-weekly), followed by acoustic (ASR) and tactile startle (TSR) with or without acoustic or light prepulses, and then on novelty tests as used by Montay-Gruel, et al.¹², radial water maze (RWM) for working memory, Morris water maze (MWM) acquisition and reversal for allocentric learning and memory and cognitive flexibility, the Cincinnati water maze (CWM-A and B) for egocentric learning and memory, MWM shift and shift reversal for follow-up spatial learning, and NOR. At the end of behavioral testing, brains were collected and analyzed for α -amino-3-hydroxy-5-methyl-4-isoxazolepropionic acid receptor (AMPA), N-methyl-D-aspartate receptor 1 (NMDA-NR1), and NMDA-NR2 in the hippocampus since these are important in allocentric learning and memory and dopamine receptor D1 (DRD1) and tyrosine hydroxylase (TH) in the neostriatum that are known to be important in egocentric learning and memory. A different set of rats was assessed for proinflammatory cytokines at post-irradiation day 2 (PID2) and PID7, since others showed changes in cytokines after electron irradiation²⁷.

Results

Two experiments were conducted: a comprehensive behavioral and cognitive assessment (Experiment 1) and a cytokine study (Experiment 2). There were 4 groups in each experiment: Sham, CV, FLASH-60, and FLASH-95. Behavioral assessment began on PID7. For the behavioral analyses, unless otherwise stated, the group sizes were as follows: Sham = 21, CV = 21, FLASH-60 = 16, and FLASH-95 = 18. Two Dunnett test comparisons were made for main effects: in the first all groups were compared with Sham and cognitive deficits were hypothesized, and in the second all groups were compared against the CV group since this is the test of FLASH sparing versus CV exposure. A timeline of the behavioral test battery for Experiment 1 is shown in Fig. 1.

Mortality and body weights

All groups started with 22 rats except for the FLASH-60 group that started with 26 rats. One rat died in the Sham and CV groups, 3 rats in the FLASH-95 group, and 10 rats in the FLASH-60 group. The FLASH-60 group had increased mortality compared with the other groups ($X^2(3) = 15.35, p < 0.002$) with most deaths occurring within 2 weeks PID (Fig. 2a).

All irradiated groups weighed less than the Sham group, $p < 0.0001$, but there were no differences between the CV and FLASH groups. Body weights of all groups increased over the weeks [$F(22, 1439) = 84.3, p < 0.0001$]. There was an interaction of irradiation \times day [$F(66, 1493) = 9.03, p < 0.0001$]. On the day of irradiation, there were no differences in body weights between groups, however beginning at PID7, irradiated groups weighed less than the Sham group ($p < 0.0001$) (Fig. 2b).

Open field

Rats were tested in the open field every other week starting at PID7 to test motor ability, explorative behavior, and general health prior to cognitive testing. Total ambulation (Fig. 3a and b) was reduced in all irradiated groups compared with Sham (Fig. 3b: CV: $p < 0.02$; FLASH-60: $p < 0.01$; FLASH-95: $p < 0.001$). There were no differences for total ambulation between the FLASH groups and the CV group. Total ambulation increased over time [$F(4, 212) = 4.34, p < 0.003$] compared with week-1 with the exception of week-5 (Fig. 3a), however, the irradiation \times week interaction was not significant. Similarly, center ambulation (Fig. 3c and d) was reduced in all irradiated groups compared with Sham (Fig. 3d: CV: $p < 0.05$; FLASH-60: $p < 0.01$; FLASH-95: $p < 0.01$), however there were no differences between CV and FLASH groups. Center ambulation also increased over weeks [$F(4, 211) = 8.45, p < 0.0001$] compared with week-1 (Fig. 3c), however, there was no interaction of irradiation \times week.

Acoustic and tactile startle response

On PID64 ASR and TSR were assessed in blocks of 5 trials across a total of 10 blocks. For ASR, only the FLASH-95 group had greater ASR than Sham [Fig. 4a: FLASH-95: $p < 0.04$], and there were no differences between the CV and FLASH groups. There was an effect of trial block [$F(9, 460) = 2.26, p < 0.02$] but not of irradiation \times block. For TSR, all irradiated groups, regardless of dose rate, had greater responses than the Sham group [Fig. 4b: CV: $p < 0.007$; FLASH-60: $p < 0.005$; FLASH-95: $p < 0.0001$]. There were no differences between the CV and FLASH groups. Block was significant [$F(9, 463) = 2.00, p < 0.04$] but not the interaction of irradiation \times block.

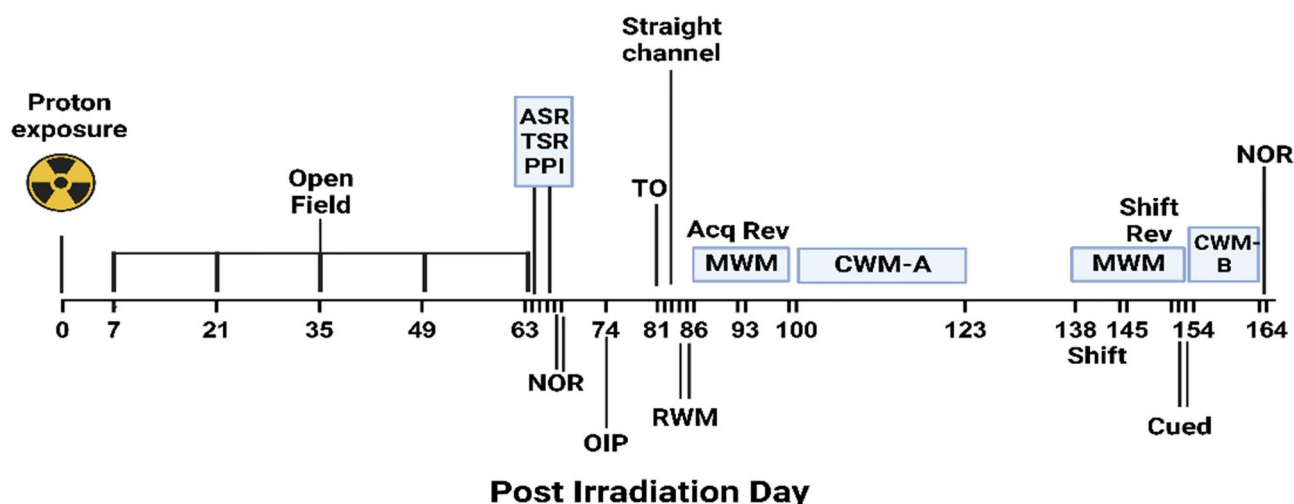


Fig. 1. Timeline of behavioral and cognitive tests. Rats were tested five times PID at two-week intervals in open field, and then for acoustic and tactile startle response (ASR and TSR) habituation and prepulse inhibition (PPI) with acoustic or light prepulses prior to ASR or TSR, novel object recognition (NOR), object in place (OIP), and object temporal order (TO). Water maze testing was next beginning with straight channel training, then radial water maze (RWM), Morris water maze (MWM) acquisition (Acq) and reversal (Rev), Cincinnati water maze (CWM-A), MWM shift, shift reversal, and MWM cued, CWM-B, and NOR. Created with BioRender.com.

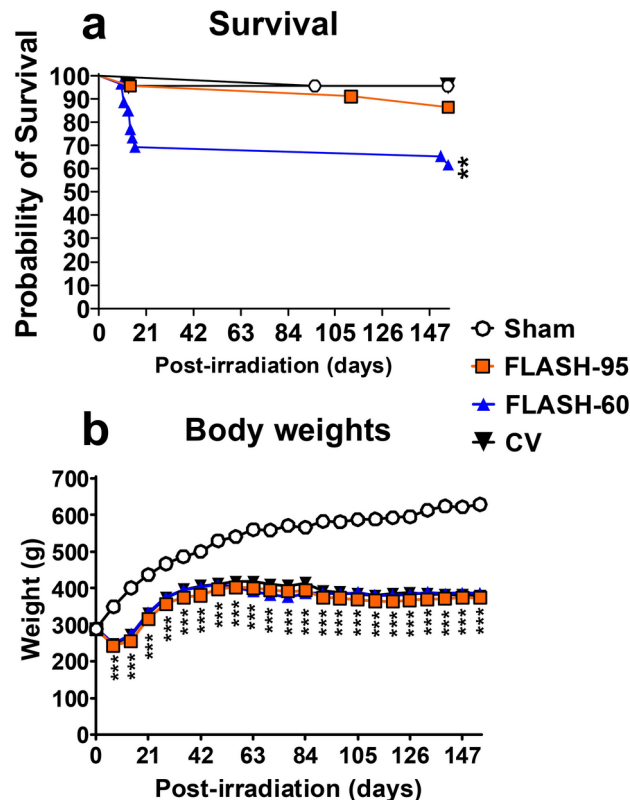


Fig. 2. Survival (a) and body weight (b) after Sham or 18 Gy cranial irradiation. Mortality was higher in the FLASH-60 group compared with the other groups ($p < 0.002$). Irradiated rats all lost weight within the first week and weight remained significantly depressed compared with the Sham group at all timepoints from PID7 until the end of behavioral testing at PID154. There were no differences in weights between the CV and FLASH groups. $**p < 0.01$, $***p < 0.001$ compared with Sham. Mortality was analyzed by log-rank Mantel-Cox test and body weights were analyzed by irradiation \times day (repeated) ANOVA. Sham = 21, FLASH-95 = 18, FLASH-60 = 16, and CV = 21.

Acoustic and light prepulse inhibition with ASR and TSR

On PID65, rats were tested for ASR and TSR with an acoustic prepulse (PPI). For ASR with an acoustic prepulse, there were no differences between groups. With each increase in sound level of the prepulse, rats had greater inhibition regardless of group [$F(4, 210) = 101.05$, $p < 0.0001$]; there was no interaction of irradiation \times trial type (Fig. 5a).

For TSR with acoustic prepulse, the CV and FLASH-95 rats had increased responses, regardless of trial type, compared with Sham rats (Fig. 5b: CV: $p < 0.04$; FLASH-95: $p < 0.003$). There was no difference between the FLASH-60 and Sham rats and no differences between the CV and FLASH groups. With each increase in the sound level of the prepulse, rats had greater inhibition [$F(4, 218) = 35.92$, $p < 0.0001$], and there was no interaction of irradiation \times trial type (Fig. 5c).

On PID66, rats were tested for ASR and TSR with a light prepulse. For ASR with light prepulse, prepulse to pulse interval was varied rather than prepulse intensity; there were no differences between irradiated groups and Sham controls or between the CV and FLASH groups. Regardless of group, the typical U-shaped curve for time-dependent inhibition was observed [$F(4, 191) = 115.60$, $p < 0.0001$]. There was an effect of irradiation \times trial type [$F(12, 226) = 2.27$, $p < 0.01$] (Fig. 5d). At the 400 ms prepulse, the 95-FLASH rats had an increased response compared with the Sham and CV groups.

For TSR with light prepulse, the FLASH-95 rats had greater TSR compared with Sham rats ($p < 0.02$), whereas there was no difference between the FLASH-60 or CV rats compared with Sham controls (Fig. 5e). There was also no difference between the CV group and the FLASH groups. However, there was an effect of irradiation \times trial type [$F(12, 288) = 1.78$, $p = 0.05$]. With no prepulse, the CV ($p < 0.03$) and FLASH-95 ($p < 0.002$) rats had a greater response than Sham rats whereas the FLASH-60 did not differ significantly from Sham. Similarly, at 400 ms the FLASH-95 ($p < 0.003$) rats had a greater response than Sham rats whereas the CV and FLASH-60 groups did not differ from Sham. Inhibition was observed at all prepulse intervals compared with no prepulse trials [$F(4, 288) = 84.39$, $p < 0.0001$] (Fig. 5f).

Novel object recognition

NOR was assessed on PID67–PID68. There were no differences in preferences for the novel object between irradiated groups and Sham or between the CV group and FLASH groups. All groups spent more time with the

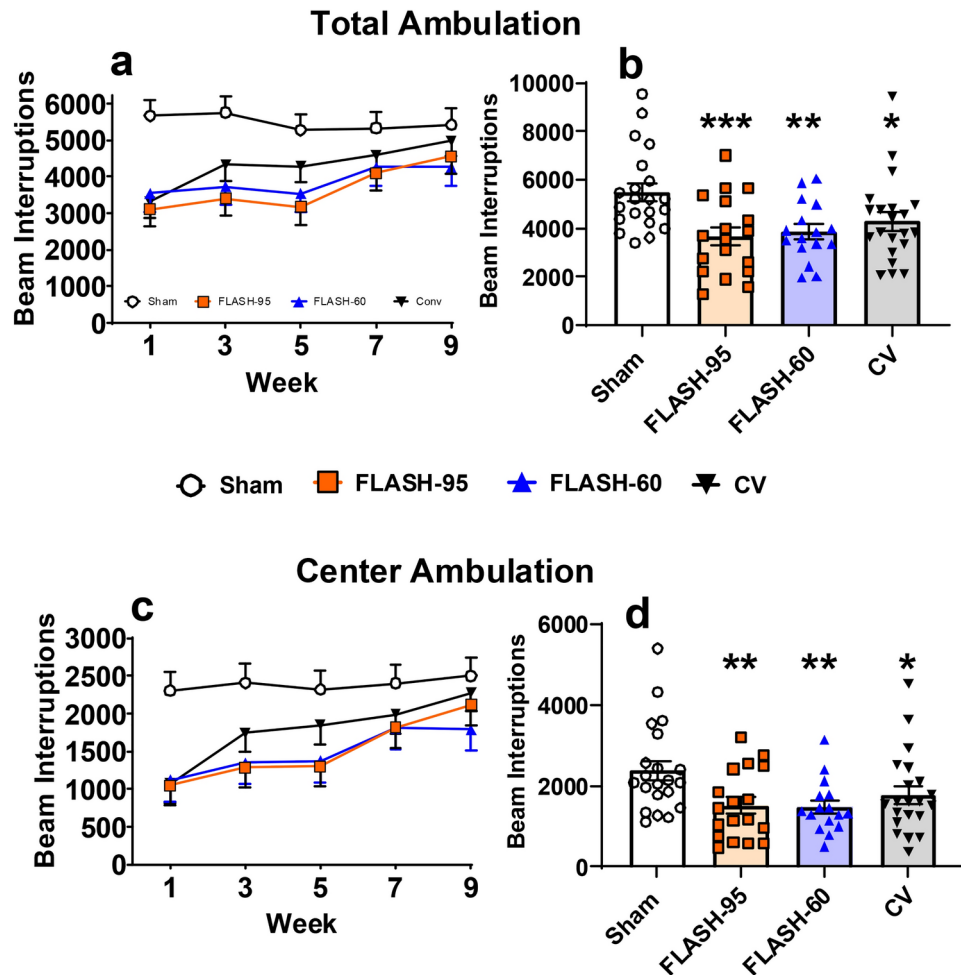


Fig. 3. Open field total activity (**a, b**) and center ambulation (**c, d**) measured in photobeam interruptions. (**a**) Total ambulation over 5 biweekly tests. (**b**) Main effect for total ambulation. All irradiated groups had reduced ambulation compared with Sham. The CV and FLASH groups did not differ for total ambulation. (**c**) Center ambulation over 5 biweekly tests. (**d**) Main effect for center ambulation. All irradiated groups had reduced center ambulation compared with Sham. Center ambulation for CV and FLASH groups was not significantly different. No interactions were significant. Open field activity was analyzed by Dunnett's and an irradiation \times week (repeated) ANOVA. * $p < 0.05$, ** $p < 0.01$, *** $p < 0.001$. Sham = 21, FLASH-95 = 18, FLASH-60 = 16, and CV = 21.

novel object compared with the familiar objects (chance = 7.5 s). Mean novel object exploration times out of 30 s were: Sham: 10.6 ± 1.0 s; FLASH-95: 11.4 ± 1.1 s; FLASH-60: 9.0 ± 1.2 s; CV: 10.5 ± 1.0 s.

Object in place

Object in place was assessed on PID74. There were no differences in preferences for the changed positions of two objects between irradiated groups and Sham or between the CV group and FLASH groups. All groups performed below chance (15 s). Mean object in place exploration times were as follows: Sham: 9.9 ± 1.3 s; FLASH-95: 11.0 ± 1.4 s; FLASH-60: 8.7 ± 1.5 s; CV: 11.6 ± 1.3 s.

Temporal order

Temporal order was assessed on PID81–PID82. There were no differences in preference for the first object versus the second between irradiated groups and Sham or between the CV group and FLASH groups. All groups preferred the first object (chance = 15 s). Mean first object exploration times were: Sham: 18.0 ± 1.4 s; FLASH-95: 16.9 ± 1.4 s; FLASH-60: 18.1 ± 1.7 s; CV: 16.7 ± 1.4 s.

Straight channel swim training

Straight channel swimming was tested on PID83. There were no differences in swim latencies between irradiated groups and Sham or between the CV group and FLASH groups. Mean latencies to reach the submerged platform were: Sham: 11.0 ± 0.7 s; FLASH-95: 13.1 ± 0.8 s; FLASH-60: 11.1 ± 0.8 s; CV: 12.9 ± 0.7 s.

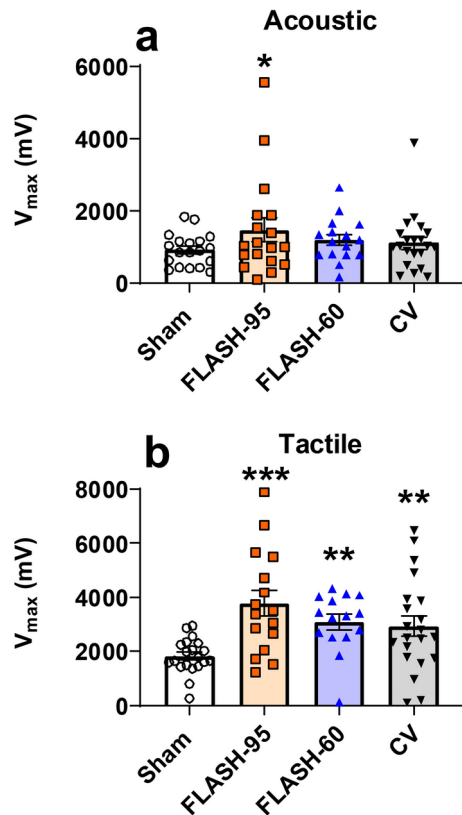


Fig. 4. Acoustic startle response (a) and tactile startle response (b) of irradiated and Sham rats. The FLASH-95 rats had increased ASR compared with the Sham rats, whereas the CV and FLASH-60 rats did not differ from Sham rats. There were no differences between the CV rats and the FLASH rats (a). All irradiated groups had increased TSR relative to the Sham group, but there were no differences between the CV and FLASH groups (b). Startle responses were analyzed by Dunnett's and an irradiation \times block (repeated) ANOVA for each pulse. * $p < 0.05$, ** $p < 0.01$, *** $p < 0.001$. Because of nonresponses group sizes were for ASR: Sham = 18, FLASH-95 = 17, FLASH-60 = 16, and CV = 20 and for TSR: Sham = 20, FLASH-95 = 16, FLASH-60 = 15, and CV = 20.

Radial water maze

Rats were tested in the RWM from PID84-PID85. On both days, irradiated rats were not impaired compared with the Sham group nor were there any differences between the CV and FLASH groups. Latency to find a submerged platform increased over trials on day 1 [$F(6, 334) = 22.54$, $p < 0.0001$] and day 2 [$F(6, 302) = 21.70$, $p < 0.0001$] as each found platform was removed. There were no significant interactions. Mean latencies to locate a hidden platform across trials on Day 1 were: Sham: 17.0 ± 1.6 s; FLASH-95: 12.5 ± 1.7 s; FLASH-60: 15.2 ± 1.8 s; CV: 13.1 ± 1.6 s. On Day 2, mean latencies were: Sham: 14.3 ± 1.4 s; CV: 9.5 ± 1.4 s; FLASH-60: 11.4 ± 1.6 s; FLASH-95: 10.5 ± 1.5 s.

Morris water maze-acquisition and reversal

The acquisition phase of the MWM was tested from PID86-PID92. There were no differences for latency to the platform during acquisition (Fig. 6a) between the Sham and irradiated groups nor between the CV and FLASH groups. All groups had decreased latencies to the platform over days [$F(5, 273) = 103.10$, $p < 0.0001$]. There was no interaction of irradiation \times day. For path efficiency, however the CV ($p < 0.05$) and FLASH-60 ($p < 0.03$) groups were less efficient at locating the platform compared with Sham, while the FLASH-95 group did not differ from Sham (Fig. 6b). No differences for path efficiency were found between the CV and FLASH groups. All groups had increased path efficiency to the platform over days [$F(5, 264) = 54.61$, $p < 0.0001$]; there was no irradiation \times day interaction. On PID92 a probe trial for reference memory was given. There were no differences between groups for average distance to the former platform site (Fig. 6c), although the FLASH-60 group approached significance for being further from the platform on average ($p < 0.06$). No differences for average distance were found between the CV and FLASH groups.

The reversal phase of the MWM was tested from PID93-PID99. The CV ($p < 0.04$) and FLASH-60 ($p < 0.004$) groups took longer to locate the platform during reversal than the Sham group, with no difference between the Sham and FLASH-95 groups (Fig. 6d). Overall, the rats located the platform faster over days [$F(5, 282) = 51.42$, $p < 0.0001$], with no interaction of irradiation \times day. Similarly for path efficiency, the CV ($p < 0.009$) and FLASH-60 ($p < 0.002$) groups were less efficient at locating the platform compared with Sham rats (Fig. 6e) with the FLASH-95 group approaching significance ($p < 0.06$). Path efficiency increased over days in all groups [$F(5,$

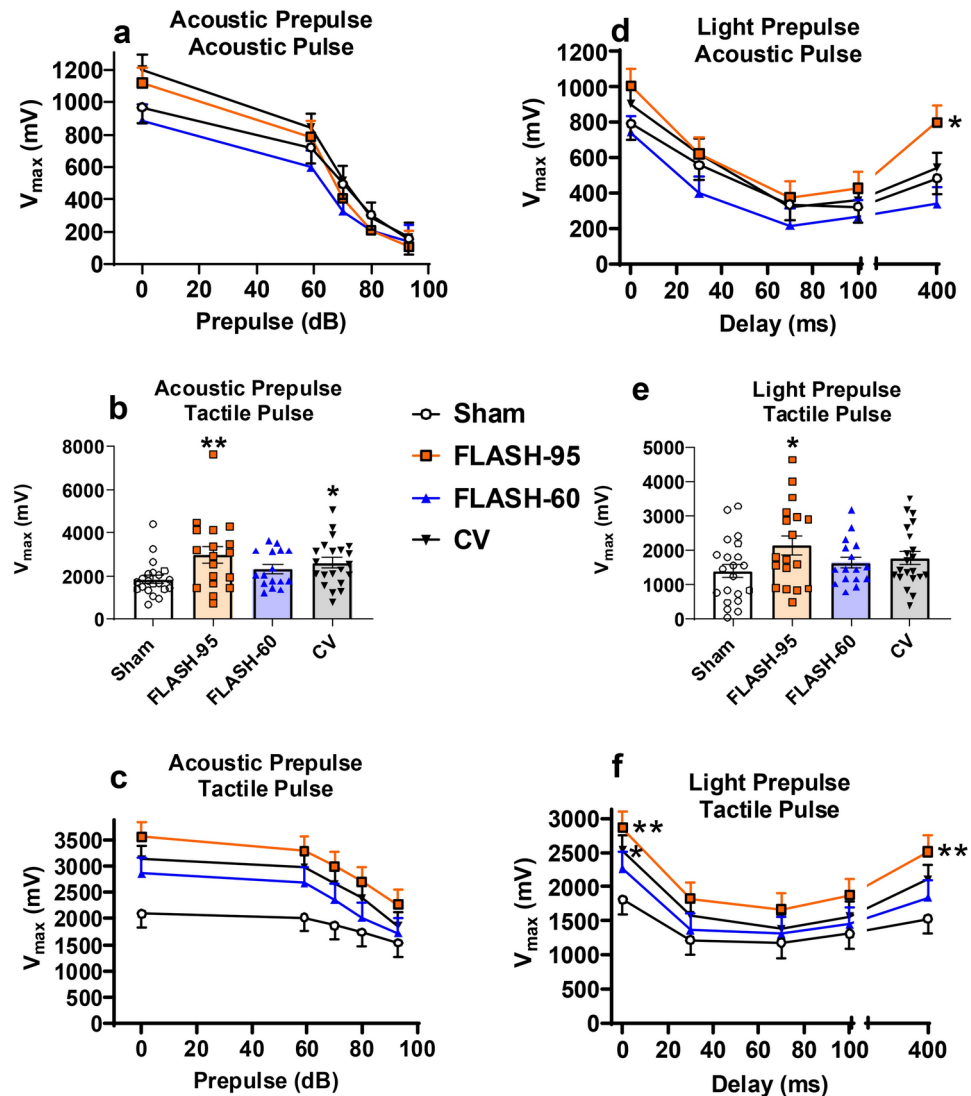


Fig. 5. Acoustic or light prepulse inhibition with ASR and TSR. Acoustic prepulse with ASR (a). Acoustic prepulse with TSR (b, c); FLASH-95 and CV rats had greater responses than Sham rats, and there were no differences between the CV and FLASH groups for ASR or TSR with the acoustic prepulse. Because of nonresponses with acoustic prepulse group sizes were for ASR: Sham = 19, FLASH-95 = 18, FLASH-60 = 16, and CV = 20 and for TSR: Sham = 21, FLASH-95 = 18, FLASH-60 = 16, and CV = 21. Light prepulse with ASR (d); FLASH-95 rats had greater responses at 400 ms compared with the Sham and CV rats. Light prepulse with TSR (e, f); FLASH-95 rats had greater responses than Sham overall. There were no differences between the CV and FLASH groups for ASR or TSR following the light prepulse (e). An interaction between irradiation and delay interval was observed such that the FLASH-95 and CV rats had higher zero-second responses and the FLASH-95 rats had higher responses at 400 ms compared with Sham (f). Startle responses were analyzed by Dunnett's and an irradiation \times prepulse type (repeated) ANOVA for each pulse. Because of nonresponses with light prepulses group sizes were for ASR: Sham = 19, FLASH-95 = 17, FLASH-60 = 16, and CV = 21 and for TSR: Sham = 21, FLASH-95 = 18, FLASH-60 = 16, and CV = 21. * $p < 0.05$, ** $p < 0.01$ versus Sham.

288) = 44.39, $p < 0.0001$], but there was no interaction of irradiation \times day. For latency and path efficiency, there were no differences between the CV group and FLASH groups. On PID99 a probe memory trial was given and there were no differences between the Sham and irradiated groups nor between the CV and FLASH groups (Fig. 6f).

Cincinnati water maze-configuration A

The CWM-A was run from PID100-PID123. For latency to escape, all the irradiated groups were slower than the Sham groups (Fig. 7a: CV: $p < 0.005$; FLASH-60: $p < 0.004$; FLASH-95: $p < 0.03$), and there were no differences between the CV and FLASH groups. All rats found the platform faster over days, [F(23, 1543) = 9.94, $p < 0.0001$: Fig. 7b]; there was an interaction of irradiation \times day [F(69, 1590) = 1.36, $p < 0.03$]. On day-9 through 18 and again from day-20 to 23, the CV and FLASH-60 groups were slower to reach the platform than the Sham group.

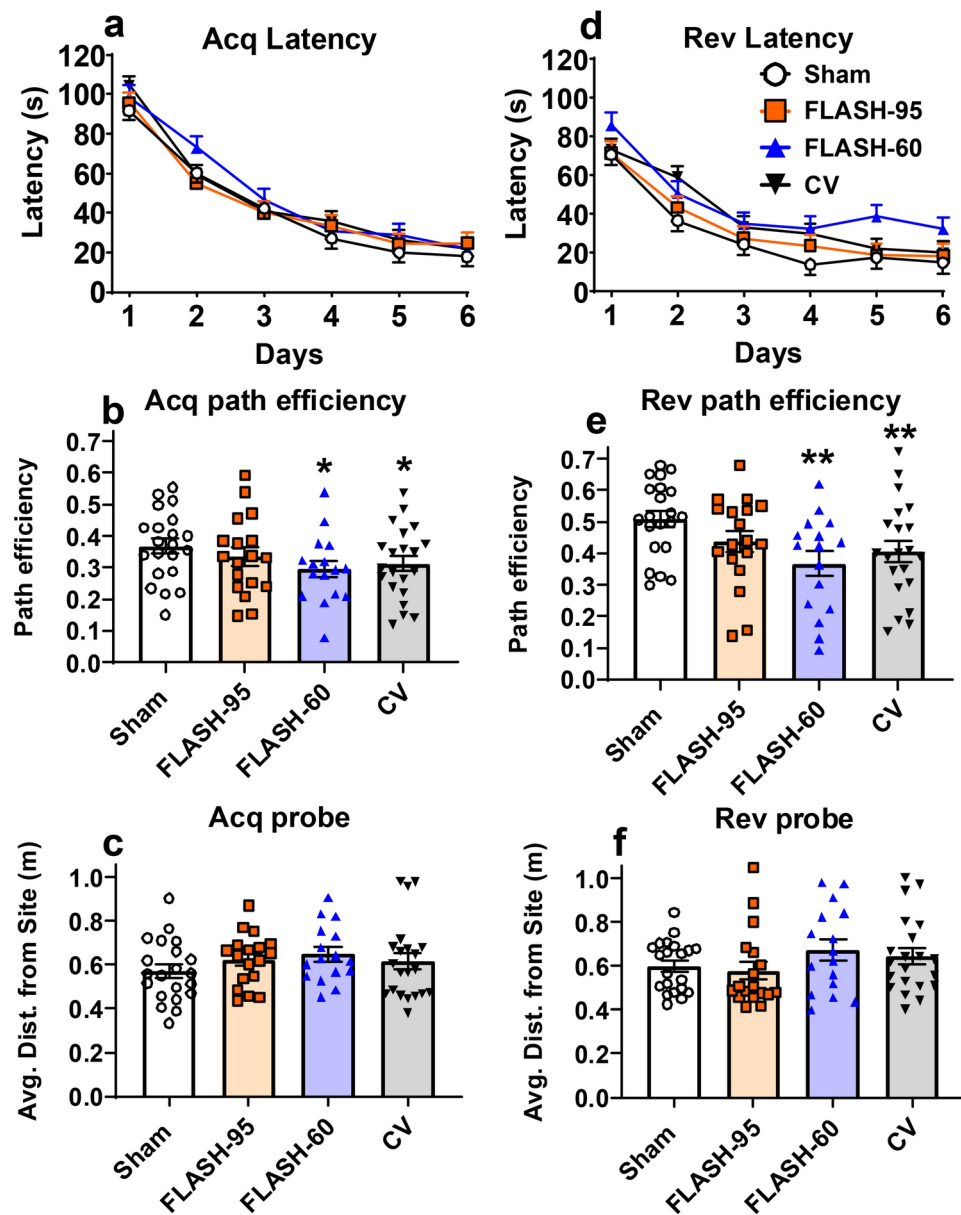


Fig. 6. Morris water maze acquisition (Acq; a–c) and reversal (Rev; d–f). Acquisition latency over days (a). There were no differences for latency. Path efficiency was lower in the FLASH-60 and CV groups compared with the Sham group (b). There were no differences during the acquisition probe trial (c). Reversal latency over days (d); there were no group differences for latency. Similar to acquisition, the FLASH-60 and CV groups were less efficient than the Sham group on reversal, whereas the FLASH-95 group did not differ from Sham controls (e), but there were no differences during the reversal probe trial (f). No differences were found during Acq or Rev between the CV rats and the FLASH rats. MWM data were analyzed by Dunnett's and an irradiation \times day (repeated) ANOVA for each phase. Sham = 21, FLASH-95 = 18, FLASH-60 = 16, and CV = 21. * $p < 0.05$, ** $p < 0.01$ versus Sham.

The FLASH-95 rats were slower to reach the platform on day-11 through 18 and again on Day-20 through 23 compared with the Sham group.

For errors all irradiated groups made more errors compared with the Sham group (Fig. 7c: CV: $p < 0.006$; FLASH-60: $p < 0.004$; FLASH-95: $p < 0.03$), but no differences were found between the CV and FLASH rats. All rats made fewer errors over days, [(F(23, 1542) = 10.58, $p < 0.0001$; Fig. 7d]; there was an interaction of irradiation \times day [F(69, 1590) = 1.43, $p < 0.02$]. The CV and FLASH-60 groups made more errors on day-7 to day-20 as well as day-22, compared with the Sham group. The FLASH-95 rats made more errors on day-7, day-11 to day-13, day-15 to day-18, day-20 and day-22 compared with the Sham rats.

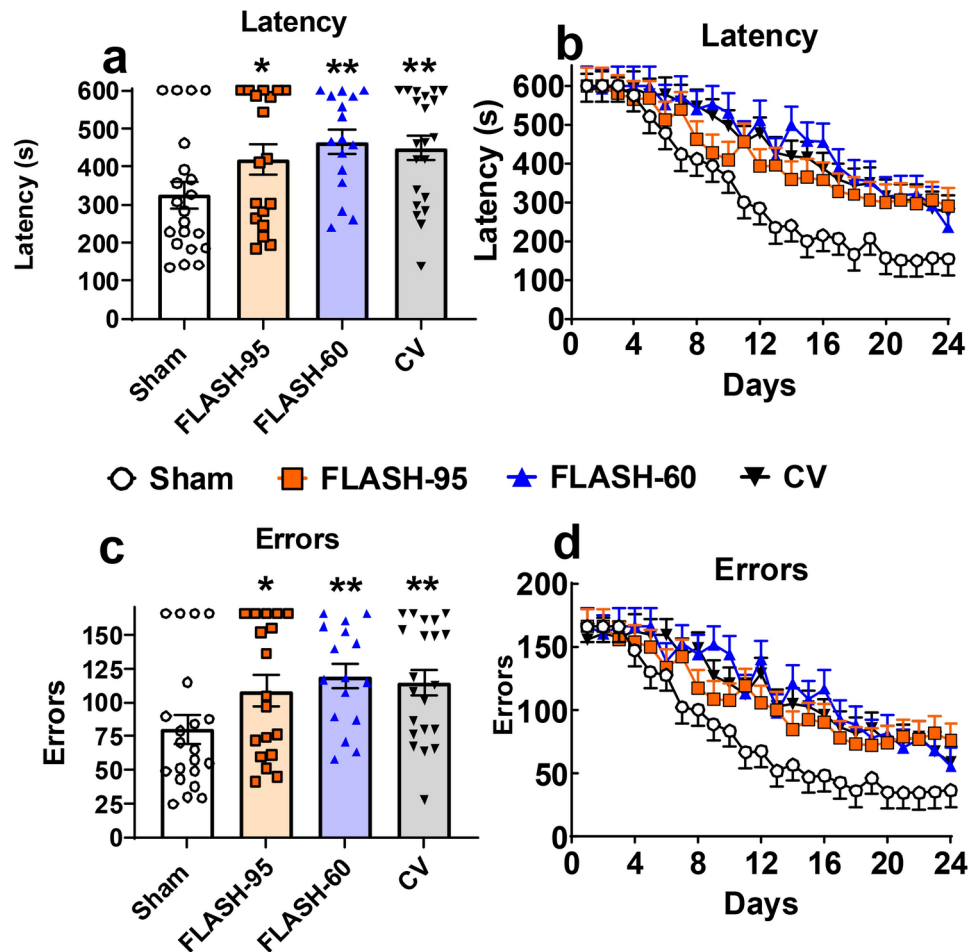


Fig. 7. The Cincinatti water maze, CWM-A latency (a, b) and errors (c, d). All irradiated groups took longer to locate the platform (a) and had more errors (c) compared with the Sham group. There were no differences in latency or errors between the CV group and the FLASH groups. The latency (b) and errors (d) over days for each group. CWM data were analyzed by Dunnett's and an irradiation \times day (repeated) ANOVA. Sham = 21, FLASH-95 = 18, FLASH-60 = 16, and CV = 21. * $p < 0.05$, ** $p < 0.01$ versus Sham.

Morris water maze-shift and shift reversal

The shift phase of the MWM was tested from PID138-PID144, 52 days after the first MWM test. All irradiated groups ($p < 0.0001$) were slower to reach the platform compared with the Sham group, but there were no differences between the CV rats and the FLASH rats. Latencies decreased over days for all groups [$F(5, 266) = 29.28$, $p < 0.0001$; Fig. 8a]. The interaction was not significant. Similarly, all irradiated groups ($p < 0.0001$) had a lower path efficiency compared with the Sham group with no difference between the CV group and FLASH groups (Fig. 8b). Path efficiency increased over days for all groups [$F(5, 288) = 29.14$, $p < 0.0001$]; there was no interaction between irradiation \times day. During the probe trial, the CV ($p < 0.01$) and FLASH-95 ($p < 0.02$) rats were on average further from the former platform site than the Sham rats, whereas the FLASH-60 rats only approached significance ($p < 0.06$) Fig. 8c. There were no differences between the CV rats and FLASH rats during the probe trial.

The shift reversal phase was tested from PID145-PID151. A similar pattern compared with the Shift phase emerged. All irradiated groups ($p < 0.0001$) were slower to reach the platform compared with the Sham group, but there were no differences between the CV and FLASH groups. Latencies decreased over days for all groups [$F(5, 286) = 27.67$, $p < 0.0001$; Fig. 8d]. The interaction was not significant. All irradiated groups ($p < 0.0001$) had lower path efficiencies compared with the Sham group, Fig. 8e. Path efficiency increased over days for all groups [$F(5, 282) = 24.68$, $p < 0.0001$] and irradiation interacted with day [$F(15, 317) = 1.78$, $p < 0.04$]. Across days, all irradiated groups performed below the Sham group (not shown). During the probe trial, the CV ($p = 0.01$), FLASH-60 ($p < 0.0005$), and FLASH-95 ($p < 0.0009$) rats were on average further from the former platform site than Sham rats (Fig. 8f). There were no differences between the CV rats and FLASH rats during the probe trial.

Morris water maze-cued

The cued phase of the MWM was run from PID152-PID153. All irradiated rats ($p < 0.0001$) took longer to locate the cued platform than the Sham group, and there was an interaction of irradiation \times day [$F(3, 72) = 9.87$, $p < 0.0001$].

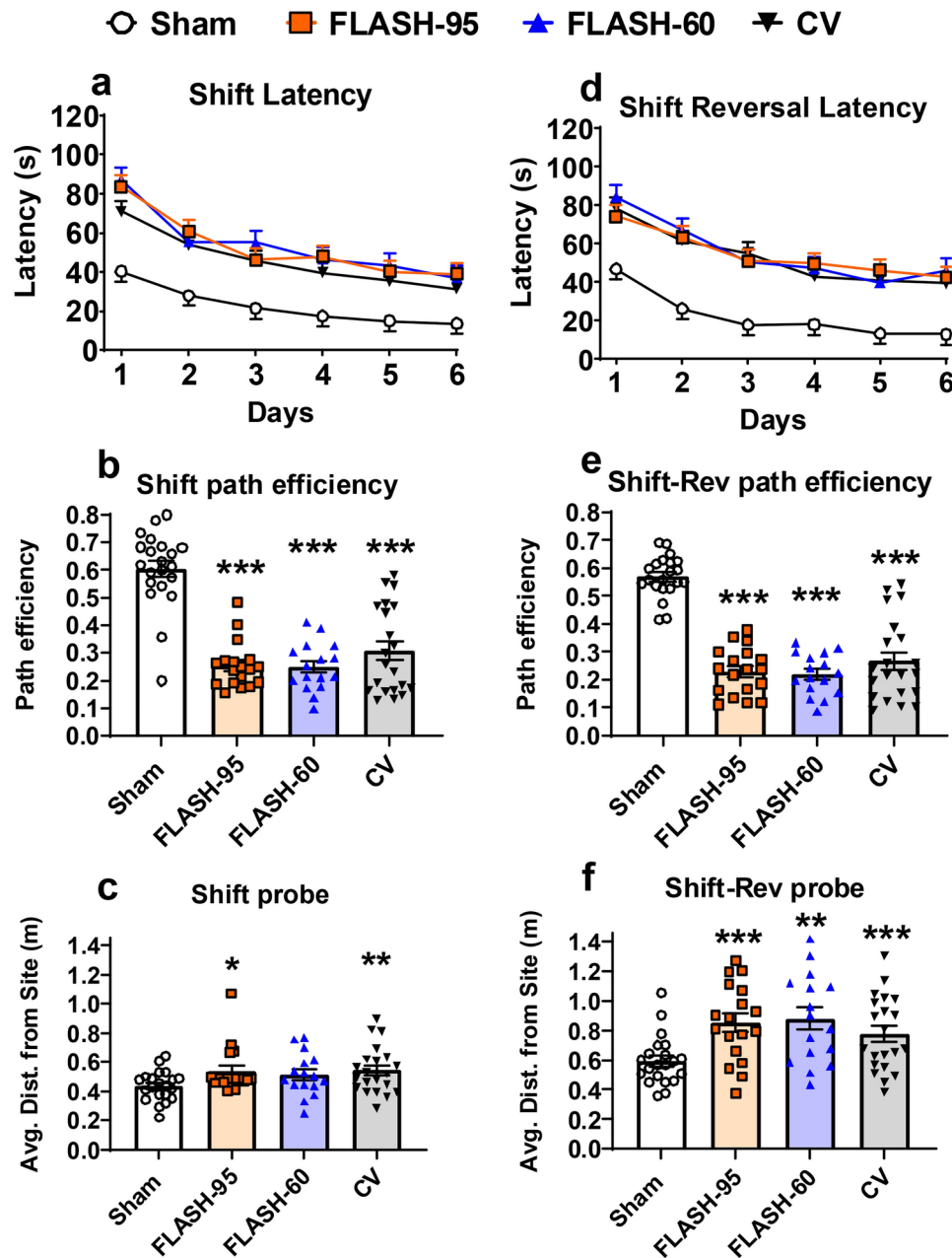


Fig. 8. Morris water maze shift (a–c) and shift reversal (d–f). Shift latency over days (a); all irradiated groups had significantly longer latencies than Sham controls. Path efficiency was lower in all irradiated groups compared with the Sham group (b). The CV and FLASH-95 groups were further from the platform on average compared with the Sham group on the probe trials (c). Reversal latency over days (d); all irradiated groups had significantly longer latencies than Sham controls. For shift reversal, all irradiated groups were less efficient than the Sham group (e), and they were further from the platform during the probe trial compared with the Sham group (f). During the shift and shift reversal phases, there were no differences between the CV rats and the FLASH rats. MWM data were analyzed by Dunnett's and an irradiation \times day (repeated) ANOVA for each phase. Sham = 21, FLASH-95 = 18, FLASH-60 = 16, and CV = 21. * $p < 0.05$, ** $p < 0.01$, *** $p < 0.001$ versus Sham.

0.0001: Fig. 9a]. All irradiated groups were slower to reach the platform than the Sham group, and the FLASH-95 group was faster than the CV group with no difference between the CV and FLASH-60 rats. The effect of day approached significance ($p < 0.06$).

Cincinnati water maze-B (CWM-B)

The CWM-B is a mirror image version of the CWM-A and was tested from PID154–PID163. For latency to the platform, all groups performed similarly and improved over days [$F(9, 558) = 16.91$, $p < 0.0001$: Fig. 9b]. There

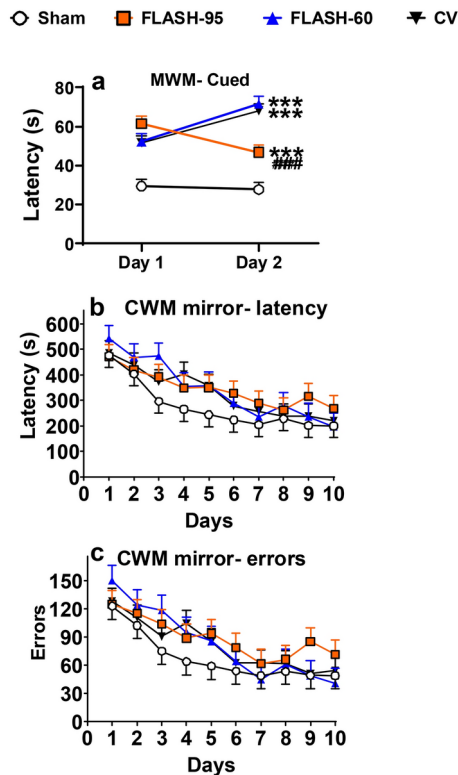


Fig. 9. Cued Morris water maze (a) and CWM-B latency (b) and errors (c). All irradiated groups took longer to locate the cued platform (a) and on Day 2 the FLASH-95 rats found the platform faster than the CV rats. There were no differences in the CWM-B latency (b) or errors (c) compared with the Sham group. MWM and CWM data were analyzed by Dunnett's and an irradiation \times day (repeated) ANOVA. Sham = 21, FLASH-95 = 18, FLASH-60 = 16, and CV = 21. *** $p < 0.001$ vs Sham, ### vs CV.

was no interaction of irradiation \times day. Similarly, for errors there were no differences between the irradiated rats and the Sham group nor the CV rats and FLASH rat. Errors decreased over days [$F(9, 558) = 17.70$, $p < 0.0001$; Fig. 9c]. There was no interaction.

Novel object recognition

The final test was NOR on PID164. Due to an error, two rats in the Sham group were not tested leaving 19 rats in this group. There were no differences in exploration of the novel object between the groups. Except for the FLASH-60 group, all groups explored the novel object near or above chance (7.5 s). Mean novel object exploration times were: Sham: 9.2 ± 1.5 s; FLASH-95: 9.6 ± 1.6 s; FLASH-60: 6.6 ± 1.7 s; CV: 7.7 ± 1.5 s.

Protein analyses

At the end of behavioral assessment, the hippocampus and neostriatum were dissected and analyzed for α -amino-3-hydroxy-5-methyl-4-isoxazolepropionic acid receptor (AMPA), N-methyl-D-aspartate receptor 1 (NMDA-NR1), and NMDA-NR2 (Fig. 10a–c) were assayed in the hippocampus and dopamine receptor D1 (DRD1) and tyrosine hydroxylase (TH) (Fig. 10d–e) were assayed in the neostriatum. In the hippocampus, the FLASH-95 group had lower levels of AMPA ($p < 0.03$), and in the neostriatum lower levels of DRD1 ($p = 0.05$) and TH ($p < 0.04$) compared with the Sham group (Fig. 10a, d, and e, respectively), while there were no differences for the CV and FLASH-60 groups for these measures compared with the Sham group. There were no differences for NMDA-NR1 or NMDA-NR2 (Fig. 10b and c) between any of the irradiated groups and Sham in the hippocampus. For the comparisons between the CV and FLASH groups, there were no differences, although the FLASH-95 group approached significance with lower levels of AMPA ($p < 0.06$).

Experiment 2 cytokine analysis

Interferon gamma (IFN- γ), interleukin 10 (IL-10), IL-13, IL-1 β , IL-4, IL-5, IL-6, keratinocyte chemoattractant/human growth-regulated oncogene (KC/GRO or CXCL1), and tumor necrosis factor α (TNF- α) were assayed on PID2 or PID7 in the hippocampus (Fig. 11) and neostriatum (Fig. 12) with 5 rats/group.

For IFN- γ there were no differences between the irradiated rats and the Sham rats. There was only a significant effect of brain region with the hippocampus (Fig. 11a) having greater levels than the neostriatum (Fig. 12a) [$F(1, 32) = 239.97$, $p < 0.0001$].

For IL-10 the hippocampus (Fig. 11b) had greater levels than the neostriatum (Fig. 12b) [$F(1, 32) = 319.34$, $p < 0.0001$], and the irradiation \times region \times day interaction was significant [$F(3, 32) = 3.17$, $p < 0.04$]. On PID2

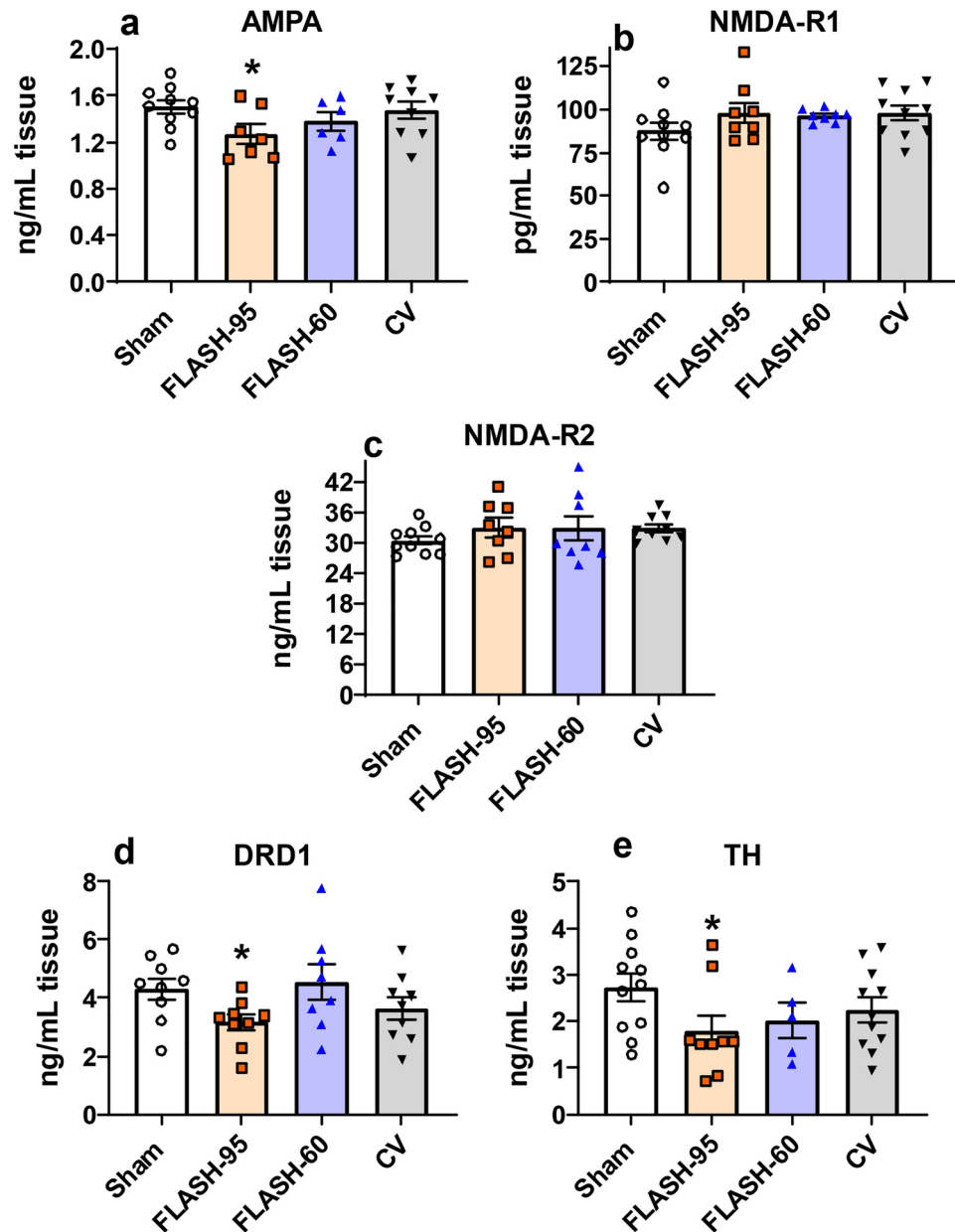


Fig. 10. In the hippocampus, AMPA (a), NMDA-NR1 (b), and NMDA-NR2 (c) were assessed by ELISA. The FLASH-95 rats had reduced AMPA levels compared with the Sham group. In the neostriatum, DRD1 (d) and TH (e) were also assessed by ELISA. The FLASH-95 rats had reduced DRD1 and TH compared with the Sham group. ELISA data were analyzed by ANOVA for each neurochemical. Sham = 9–11; FLASH-95 = 7–9; FLASH-60 = 5–8; CV = 9–11. * $p < 0.05$ versus Sham.

the CV rats had decreased IL-10 in the neostriatum compared with the Sham rats and with the FLASH-95 rats. No other differences were found.

For IL-13 the hippocampus (Fig. 11c) had greater levels than the neostriatum (Fig. 12c) [$F(1, 32) = 284.05$, $p < 0.0001$], and irradiation \times region \times day interaction was significant [$F(3, 32) = 2.98$, $p < 0.05$]. None of the irradiated groups differed from Sham rats in either region on either day, however the FLASH-95 rats had increased IL-13 compared with the CV rats on PID2 ($p < 0.03$).

For IL-1 β the hippocampus (Fig. 11d) had greater levels than the neostriatum (Fig. 12d) [$F(1, 32) = 363.03$, $p < 0.0001$], and the irradiation \times region \times day interaction was significant [$F(3, 32) = 2.89$, $p = 0.05$]. None of the irradiated groups differed from the Sham group in either region on either day. The FLASH groups had greater levels of IL-1 β in the neostriatum on PID2 compared with the CV group ($p < 0.02$).

For IL-4 there were no differences between the irradiated rats and the Sham rats, nor the CV rats from the FLASH rats. The hippocampus (Fig. 11e) had higher levels than the neostriatum (Fig. 12e) [$F(1, 32) = 379.81$, $p < 0.0001$]. No other differences were detected.

Hippocampus

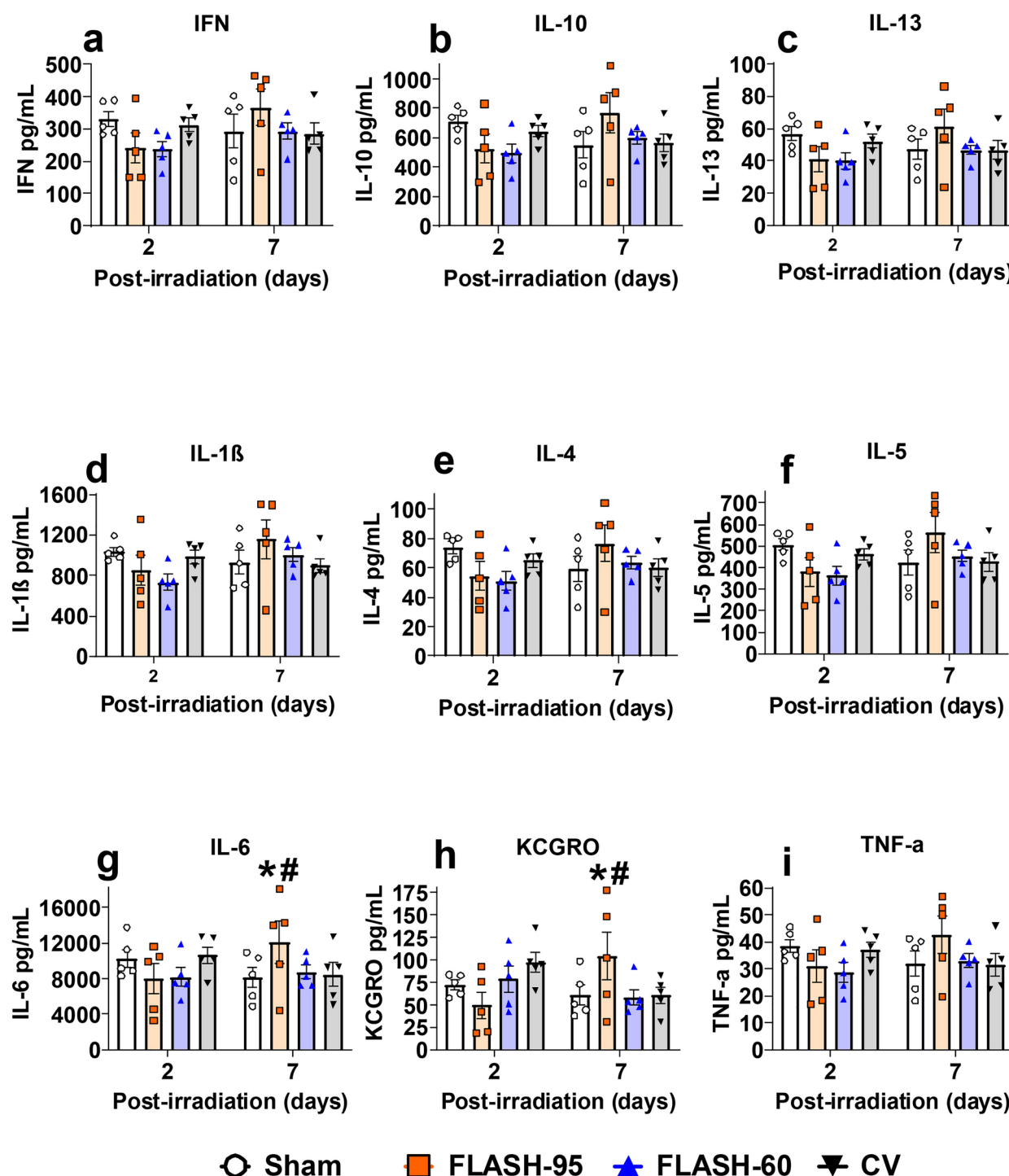


Fig. 11. Cytokines in the hippocampus of Sham, FLASH-95, FLASH-60, and CV rats either 2 or 7 days after irradiation. Cytokine data were analyzed with an irradiation \times day \times region (repeated measure) ANOVA for each cytokine. Cytokines assayed were: IFN- γ (a), IL-10 (b), IL-13 (c), IL-1 β (d), IL-4 (e), IL-5 (f), IL-6 (g), KCGRO (h), and TNF- α (i). $N = 5/\text{group/day}$. * $p < 0.05$ versus Sham # $p < 0.05$ versus CV.

For IL-5 the hippocampus (Fig. 11f) had greater levels than the neostriatum (Fig. 12f) [$F(1, 32) = 270.81, p < 0.0001$], and irradiation \times region \times day interaction was significant [$F(3, 32) = 3.25, p < 0.04$]. However, none of the irradiated groups differed from the Sham rats in either region or on either day. Similarly, there were no differences between the CV rats and the FLASH rats.

Striatum

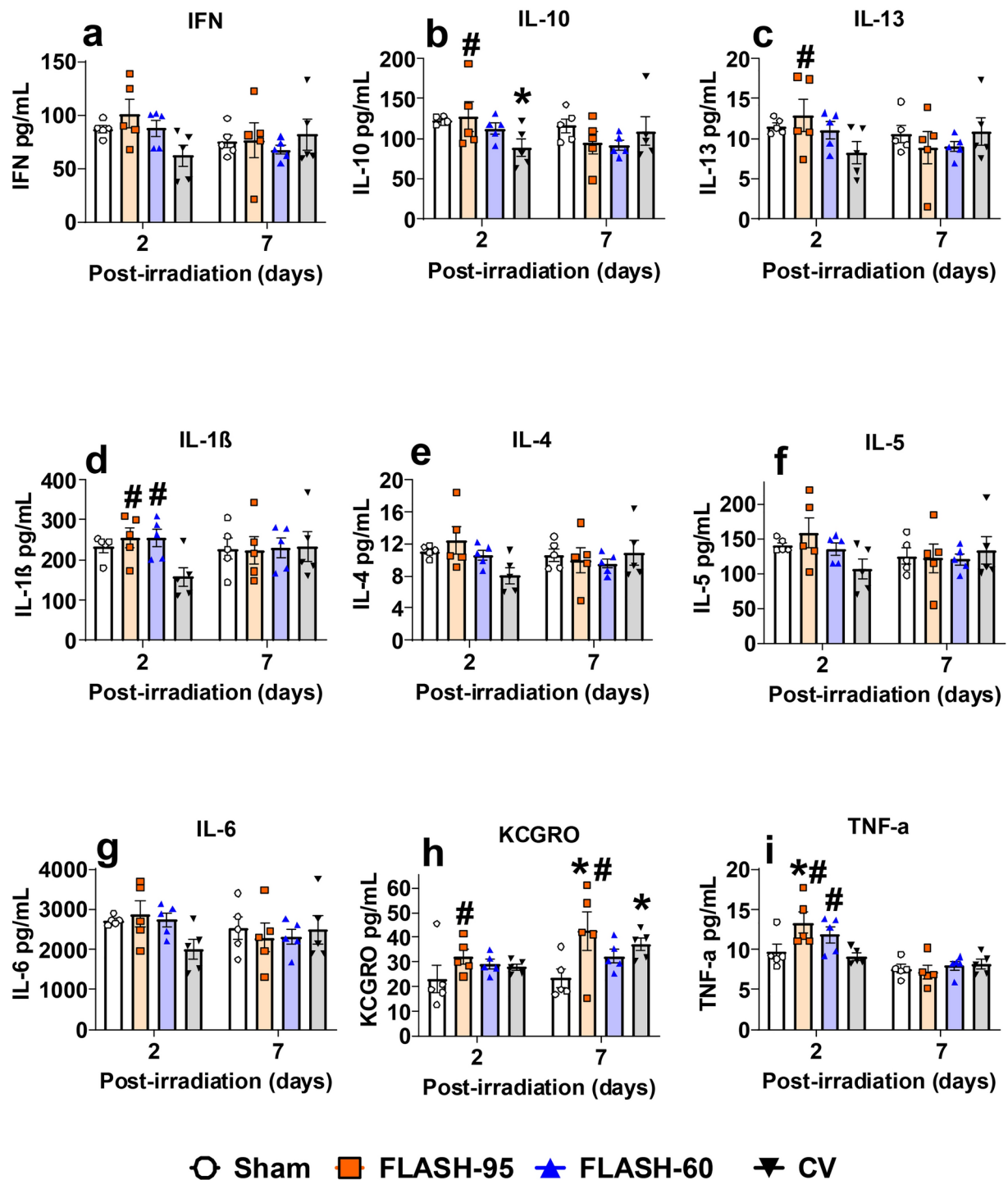


Fig. 12. Cytokines in the neostriatum of Sham, FLASH-95, FLASH-60, and CV rats either 2 or 7 days after irradiation. Cytokine data were analyzed with an irradiation \times day \times region (repeated measure) ANOVA for each cytokine. Cytokines assayed were: IFN- γ (a), IL-10 (b), IL-13 (c), IL-1 β (d), IL-4 (e), IL-5 (f), IL-6 (g), KCGRO (h), and TNF- α (i). $N = 5/\text{group/day}$. * $p < 0.05$ versus Sham # $p < 0.05$ versus CV.

For IL-6 the hippocampus (Fig. 11g) had greater levels than the neostriatum (Fig. 12g) [$F(1, 32) = 203.50$, $p < 0.0001$], and there was an irradiation \times region \times day interaction [$F(3, 32) = 3.04$, $p < 0.04$]. The FLASH-95 rats had greater IL-6 compared with the Sham rats and the CV rats in the hippocampus on PID7. There were no other differences between the Sham rats or the CV rats.

For KC/GRO the hippocampus (Fig. 11h) had greater levels than the neostriatum (Fig. 12h) [$F(1, 32) = 57.27, p < 0.0001$], and there were irradiation \times day [$F(3, 32) = 4.77, p < 0.008$] and irradiation \times region \times day interactions [$F(3, 32) = 2.99, p < 0.05$]. For the analysis of irradiation \times day effect, the FLASH-95 rats had greater KC/GRO on PID7 compared with the Sham group and greater levels on both days compared with the CV group. For the analysis of the irradiation \times region \times day effect, the FLASH-95 rats had greater KC/GRO in the hippocampus and neostriatum on PID7 compared with the Sham rats, whereas the CV rats had greater levels in the neostriatum only on PID7 compared with the Sham rats. No other differences were detected.

For TNF- α the hippocampus (Fig. 11i) had greater levels than the neostriatum (Fig. 12i) [$F(1, 32) = 254.45, p < 0.0001$], and there was an irradiation \times region \times day interaction [$F(3, 32) = 3.02, p < 0.05$]. The FLASH-95 rats had greater TNF- α compared with the Sham and CV rats in the neostriatum on PID2. The FLASH-60 rats had greater TNF- α compared with the CV rats in the neostriatum on PID2. There were no other differences.

Discussion

The assessment of cognitive dysfunction in rodents requires examination of numerous cognitive domains similar to how testing in humans is done. In this regard, we selected a range of cognitive tests that assessed working, reference, egocentric, and recognition learning and memory, executive function, preattention, as well as tests of general health such as locomotor exploration and startle to better understand the impact of cranial irradiation with protons at conventional and FLASH dose rates on the rodent brain. With the exception of cued platform in the MWM, the FLASH groups performed similarly to the CV groups on the behavioral outcomes showing impairment relative to Shams.

The FLASH-60 group of rats had greater mortality than the other groups, and most of the deaths occurred within 3 weeks of irradiation. The underlying mechanism for this is unknown. All irradiated groups had a similar decrease in body weights within a week of exposure, with some rebound observed over the following 2 weeks. Since all irradiated groups were similar in weight, lack of food intake is unlikely to explain the higher mortality rate in the FLASH-60 group. To determine if the increased mortality could be replicated, a new set of rats from the same supplier was irradiated with either 18 Gy CV or FLASH-60 ($n = 12/\text{group}$) and mortality measured through PID60. The FLASH-60 increase in mortality was not reproducible since only one FLASH-60 rat died compared with no deaths in the CV group. The cause of this difference in mortality in the main study was unknown and not reliable. While there may be some concern that a survivor bias occurred in the main study FLASH-60 group, the similarity in most of the behavioral outcomes for the FLASH groups suggest otherwise.

Increases in startle responses were observed for the acoustic stimulus in the FLASH-95 rats and for the tactile stimulus in all irradiated rats compared with Sham controls. The pathway for acoustic startle begins at the cochlear root neurons that project to giant neurons in the caudal pontine reticular nucleus that in turn synapse onto motor neurons²⁸. While disruption of this pathway results in a decreased startle response, the significance of an increased response is unknown, however it may involve the inferior colliculus which can modulate the magnitude of the startle response. For example, lesions of the inferior colliculus result in increased acoustic startle responses in mice 7 and 14 days after the lesion²⁹. Lesions of the inferior colliculus in rats inhibited prepulse inhibition, i.e., the lesioned rats had greater responses, i.e., less inhibition³⁰. The use of the collimator in this study may have spared the direct startle reflex pathway, since brainstem regions would have had reduced radiation exposure in the present experiment, but it may still have had effects on the inferior colliculus. Further experiments are required to determine if the inferior colliculus is mediating the increased startle after proton irradiation.

Hippocampal mediated spatial learning and memory dysfunction was seen in all irradiated groups with no sparing by FLASH at 18 Gy. During the acquisition and reversal phases in the MWM, none of the irradiated rats differed from Sham rats in latency to reach platform, however the CV and FLASH-60 rats did show reduced path efficiency. It appeared that the FLASH-95 group had sparing of spatial learning and memory deficits caused by proton exposure compared with the Sham group, but there was no statistically significant difference between the FLASH-95 and CV groups. When these rats were tested weeks later in the shift and shift reversal phases of the MWM, significant deficits in latency to the platform and path efficiency were observed in all irradiated groups compared with Sham rats. Hippocampal damage reliably produces deficits in spatial learning and memory^{31,32}. The hippocampus is also known to be radiosensitive, and whole brain irradiation with protons affects hippocampal function as demonstrated by deficits in the MWM⁵ and neither of the FLASH groups demonstrated signs of sparing on this test. Interestingly, the hippocampus is also important for novel object recognition³³, and mice treated with whole brain electron irradiation showed less severe deficits in NOR and related tests of novelty after FLASH versus conventional dose-rate treatment^{12,15–17,27}. However, with protons in rats no deficits in NOR were seen after FLASH or conventional dose rates^{5,19}. One of the biggest differences between the mouse and rat studies is that the time with the objects during familiarization was controlled for in the rat studies (i.e., 30 s), but varied in the mouse studies that did not include a control for time spent with objects. This is relevant because Clark, et al.³³ showed that novelty begins to wane within ~ 10 s of object exploration, therefore novelty tests only provide a limited assessment of learning ability and is predicated on an inherently fleeting tendency to notice something new in the environment for a few seconds before it becomes background. Whereas tests such as the MWM require learning over days and trials and provide a learning curve to determine rate of learning as well as the level of learning, including memory of that learning over time. The large impairments in the MWM and lack of a deficit in NOR suggests that NOR is not very sensitive for assessing learning after brain irradiation.

The CWM was used to assess egocentric learning and memory. When the CWM is run under infrared lighting, learning is largely dependent on the striatum, especially dopaminergic cells within this region^{34–36}. The striatum has neurons sensitive to boundaries called egocentric boundary neurons³⁷, and this constitutes evidence for striatal involvement in egocentric learning. In this study, two configurations of the CWM were used. In the CWM-A, all irradiated rats performed worse than Sham controls with comparable impairments to previous

studies of rats treated with cranial irradiation with protons when tested as adults or after P11 exposure^{5,19}. However, no sparing from learning impairment was found in the FLASH groups in the present study or in the P11 study in the CWM-A¹⁹. However, in the P11 study a sparing effect of FLASH was observed in the CWM-B after 5 Gy cranial irradiation. Based on the learning curve of CWM-B from the P11 study, rats in this study were tested for 10 days as well, but no differences in performance were observed between irradiated rats and Sham rats. Examination of the learning curves for CWM-A shows progressive improvements in performance from day-1 through day-10, then performance improved again around day-16 (Fig. 7b). The learning curve during the CWM-B showed steady improvement from day-1 to day-6, but then plateaued with no further improvement. Therefore, longer testing in the CWM-B may be required to detect effects since asymptotic performance was not reached. Alternatively, it may be that differences in protocols for cognitive testing, the timing of exposure to proton irradiation, or other factors were responsible for the lack of effect in the CWM-B. Consistent with the changes in the neostriatum, locomotor behavior was impaired in the irradiated groups, further supporting injury to the neostriatum after 18 Gy without sparing by FLASH.

The mechanism for the deficits following whole brain irradiation is unknown but it has been suggested to be related to neuroinflammation. In this study, radiation treatment did not result in any clear pattern of change in proinflammatory cytokine concentrations in the hippocampus or neostriatum at the two timepoints tested, 2 and 7 PID. Significant changes observed compared with Sham include a reduction in IL-10 at PID2 and increase in KC/GRO at PID7 in the neostriatum of the CV group compared with Sham. The FLASH-95 rats had increased IL-6 in the hippocampus and KC/GRO in the hippocampus and neostriatum at PID7, and increased TNF- α at PID2 in the neostriatum compared with Sham. No differences were noted between the FLASH-60 rats and Sham for any of the cytokines. While there were a number of cytokine differences between the CV and FLASH groups (Fig. 11 and 12), the lack of behavioral differences between the CV and FLASH groups makes it difficult to understand the significance of these changes. In contrast to the current study, increases in IL-1 β , TNF- α and KC/GRO were reported in studies of mice treated with cranial electron irradiation compared with unexposed controls regardless of the dose rate, and IL-4 and IL-6 were increased only in mice that received a conventional dose rate compared with FLASH treated or untreated mice²⁷. In the present study, only the FLASH-95 group had changes in TH, DRD1, and AMPA compared with the Sham rats. This is in contrast with prior data on adult rats treated with cranial irradiation with protons at a conventional rate, in which TH levels in the neostriatum decreased after 14 Gy and DRD1 decreased after 17 Gy⁵. Despite the observed differences in the effect of cranial irradiation on neurochemical levels in these two studies, many of the behavioral outcomes were similar. It is unclear why disparate neurochemical changes were observed among groups with similar behavioral outcomes, but this finding suggests that other factors such as changes to synaptic plasticity or structure may be responsible for the behavioral changes observed after cranial irradiation^{17,27}.

One limitation of this study is the use of only male rats; female rats may have different responses than males. Another limitation is the use of a single radiation dose. We selected 18 Gy as a dose that would yield behavioral deficits, and this dose is likely above the threshold to unmask a protective effect of FLASH, consistent with an upper threshold of 12–14 Gy from the murine studies using electrons^{15,16}. A study with a range of doses at different dose rates would be ideal but is challenging because of the complexity and resources needed for the battery of cognitive testing used here. The treatment technique used in this study may also have affected the results. Rats were treated with a single posterior-anterior transmission beam exposing the whole brain but also treating the entire oral cavity and most of the oropharynx. This treatment is known to cause mucositis which likely contributed to the significant weight loss experienced by all treated rats in both FLASH and CV groups, and this mucositis and weight loss may be a complicating factor in this study that was not present in studies of electron FLASH in mice. Lastly, while we were mostly concerned with cognitive effects, other types of behavioral domains could be assessed such as anxiety and depression-related behaviors. Examination of release of neurochemicals or synaptic plasticity may provide further insight into the behavioral deficits observed herein.

In conclusion, these data demonstrate that in addition to the hippocampus, the neostriatum and potentially the inferior colliculus are regions of the brain that are sensitive to radiation. FLASH treatment in this study did not result in reduced cognitive toxicity after 18 Gy cranial proton irradiation. It is unclear if this is due to radiobiological differences between protons and electrons, utilization of a dose outside of the therapeutic window, confounding effects of weight loss, or other factors. Future studies should address these variables while including a range of assessments of behavioral domains as was done here to better characterize the effects of proton radiotherapy and the FLASH effect.

Materials and methods

Subjects were Sprague Dawley CD, IGS male rats (strain #001, Charles River, Raleigh, NC) that arrived on P60 and were initially pair-housed in polysulfone cages (46 cm × 24 cm × 20 cm) in the Alternative Design (Siloam Spring, AR) MACS Flex-air wall mount system with HEPA filtered air supplied at 30 air changes/h and reverse osmosis filtered, UV purified water provided from a Lixit system (SE Lab Group, Napa, CA) at the Cincinnati Children's Hospital Medical Center (CCHMC) vivarium that is AAALAC International-accredited and pathogen free. Rats were treated in accordance with protocols approved by the CCHMC Institutional Animal Care and Use Committee protocol # 2020-0017. All experiments were performed in accordance with relevant guidelines and regulations and adhered to ARRIVE guidelines. For proton irradiation, rats were transported to the Cincinnati Proton Therapy Center's vivarium four days prior to exposure and housed in PET plastic cages (43 cm × 34 cm × 20 cm) with an Innocage external bottle system (Innovive, San Diego, CA). All cages contained woodchip bedding, a stainless-steel hut for enrichment³⁸, and had ad libitum access to NIH-07 rat chow (LabDiet #5018, Richmond, IN). Temperature (21 ± 1 °C), humidity (50 ± 10%), and light–dark cycle (14:10 h, lights on at 600 h) were automatically regulated. Rats were returned to the CCHMC vivarium three days after irradiation

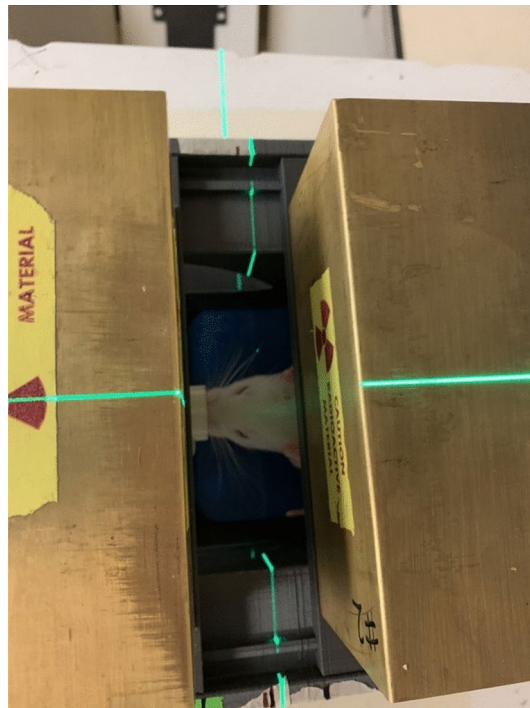


Fig. 13. Experimental setup with continuous anesthesia and the collimator in place. The gantry-mounted laser alignment system is visible for irradiation guidance.

and housed as described above with all rats in the same room and positioned on the holding rack in a counter-balanced fashion.

Proton irradiation groups

A random number table was used to determine group membership for each cohort of rats, and rats were individually identified by ear-punch prior to irradiation. There were 3 groups that had cranial irradiation at 18 Gy protons delivered at a conventional dose rate of 1 Gy/s (CV) or FLASH dose rates of 60 Gy/s (FLASH-60) or 95 Gy/s (FLASH-95), with sham treated controls for comparison (Sham: anesthetized with isoflurane and placed under the beam nozzle but not irradiated). For the behavioral study, there were 11 cohorts of rats that were irradiated with at least 2 rats from each group represented in each cohort. A total of 22 rats were irradiated in each group except for the FLASH-60 group that had 26 rats irradiated. For the cytokine study, there were 2 cohorts of rats with 6 rats per group per cohort of which 5 per group were used for cytokine assessment (48 total rats). The ProBeam Pencil Beam Scanning Gantry (Varian Medical Systems, Palo Alto, CA, USA) was used to deliver a monoenergetic, single-layer posterior-anterior transmission radiation field, such that the entire head and brain were irradiated with the entrance region of the Bragg peak. FLASH dose rates were delivered at 250 MeV, while conventional dose rates were delivered at 245 MeV. Details of proton delivery, dosimetry, and monitoring are as described⁸. Rats were anesthetized with 2–4% isoflurane mixed with room air using the SomnoSuite system (Kent Scientific, San Diego, CA). Once anesthetized, rats were placed in a prone position in a stereotaxic-like rig with a tooth bar, anesthesia nose cone, and brass collimator above to reduce proton transmission to regions outside of the head (Fig. 13). Field flatness, symmetry, and location were quality assured using gafchromic film prior to irradiation. Absolute doses and dose rates were calibrated using a NIST-traceable parallel plate ionization chamber. Dose calculation data using ionization chambers were performed using the dose-to-water formulism as reported in the IAEA TRS 398. All doses reported are physical doses and no corrections were made for relative biological effectiveness. The absolute dose and dose rate tolerances were 3% and 5%, respectively. The methodology of measuring doses in an ultra-high dose rate environment was validated using independent dose-rate invariant detectors³⁹. The dose is measured for each irradiation of each rat using a parallel-plate ion chamber and electrometer. The dose rate is calculated using the ratio of the measured dose and the irradiation time from the machine log files. This dose rate is the field dose rate and is the nominal dose rate. Additionally, a voxel-based dose rate calculation is also reported, as the PBS dose rate⁴⁰. The nominal dose rate of 60 Gy/s coincides with a PBS dose rate of 100 Gy/s, and the nominal dose rate of 95 Gy/s coincides with a PBS dose rate of 160 Gy/s. Since the FLASH radiation biology field has not settled on a consensus dose rate definition, both dose rates are reported. For this study, the proton beam is generated using a cyclotron operating at 72 MHz. This results in negligible intra-pulse dose rate and inter-pulse time structures. This beam structure is very unlike electron beams, for which time between pulses and intra-pulse dose rate is quite significant, and potentially FLASH-effect altering. Using the spot scanning delivery, the entire cranium including the whole brain was uniformly irradiated with a spot pattern that corresponds to a rectangular 2.5 cm × 3.0 cm field. The

gantry-mounted laser alignment system was used to localize the brain of each rat using anatomical landmarks, such that the inferior edge of the field and the inferior/posterior edge of the rat brain were aligned. For the purposes of this study, the dose rates reported are defined as the total dose divided by the total irradiation time, knowing that the instantaneous dose rates are 5–8 times higher.

After exposure, rats recovered from anesthesia prior to being returned to their home cage. Napa Nectar pouches (Systems Engineering Lab Group, Napa, CA) were supplied in cages as a secondary source of hydration until PID60.

Experiment one: behavioral assessment

The behavioral test battery started on PID7 (Fig. 1). Rats were tested in an open field until PID63 once every other week followed by acoustic and tactile startle habituation and prepulse inhibition (PPI) beginning on PID64. Rats were then tested in novel object recognition (NOR), object in place (OIP), and temporal order (TO). Water maze testing followed with straight channel swim training first and then radial water maze (RWM), Morris water maze (MWM) acquisition and reversal, Cincinnati water maze (CWM-A), MWM shift, shift reversal, and cued, CWM-B (mirror image version), and NOR. Rats were tested in the Animal Behavior Facility (RRID:SCR_022621) at CCHMC by personnel who were blinded to group membership.

Open field

On PID7, 21, 35, 49, and 63 rats were tested in open field for exploratory behavior for 60 min in PAS activity system (41 cm × 41 cm: San Diego Instruments (SDI), San Diego, CA) as described⁴¹. Beam-break data were recorded from an array of 16 × 16 infrared beams in 5 min intervals. Dependent measures were total and center ambulation with ambulation measured as two or more consecutive beam breaks.

Acoustic and tactile startle responses

ASR and TSR were measured the day after open-field on PID64 in SR-LAB system inside sound-attenuating test chambers (SDI) as described⁴². Rats were placed in acrylic cylindrical holders (SDI large enclosure) mounted on a platform with a piezoelectric accelerometer attached underneath. The test chamber light and fan (55 dB background noise) were turned on and the rats were adapted 5 min prior to testing. For ASR the pulse was a 20 ms, 120 dB SPL mixed frequency white noise burst (rise time 1.5 ms). For TSR the pulse was a 20 ms, 60 psi air-puff directed at the dorsum of the rat through plastic tubing. The recording window began at the onset of the pulse and lasted 100 ms. Rats were given 5 acoustic (120 dB) trials alternating with 5 tactile (60 psi) trials for a total of 50 trials of each type. Movement detected at the start of each trial was subtracted from the maximum startle amplitude (V_{\max}) to eliminate non-startle movement artifacts. A $V_{\max} < 95$ mV was considered a nonresponse for that trial and the data were excluded. The dependent variable was V_{\max} measured in mV.

Acoustic prepulse inhibition of startle

On PID65 rats were tested for ASR and TSR, using the same conditions as above, except there was an acoustic prepulse prior to the acoustic or tactile pulses as described⁴³. Briefly, the prepulses were 0, 59, 70, 80, or 93 dB SPL mixed frequency white noise burst that preceded the pulse by 70 ms from onset to onset and each prepulse lasted 20 ms. Rats received a 10 × 10 Latin square sequence of 5 trial types for ASR alternating with TSR and this was repeated twice. There were 20 trials of each prepulse and pulse combination. If the unmodified $V_{\max} < 95$ mV for a block of 5 trials, then data for all trials of that type (ASR or TSR) within that block were removed from the analyses. V_{\max} was the dependent measure.

Light prepulse inhibition of startle

On PID66 rats were tested for ASR and TSR PPI as above, with two exceptions: (1) house lights were off at the beginning of the test and (2) before the acoustic or the tactile pulse there was a light prepulse presented at interstimulus intervals of 0, 30, 70, 100, or 400 ms before the pulse as described⁴³. An LED array of high intensity lights (SDI) provided approximately 1110 ± 17 lx (mean ± SEM) visible light prepulse measured at the level of the animal holder with a light meter (Extech Easyview 33, Boston, MA). A 10 × 10 Latin square of each prepulse/pulse type was repeated until 20 trials of each were obtained. If the unmodified $V_{\max} < 95$ mV for a block of 5 trials, then data for all trials of that type (ASR or TSR) within that block were removed from the analyses. V_{\max} was the dependent measure.

Novel object recognition

On PID67–68 NOR was tested in acrylic AnyBox apparatus (40 cm × 40 cm × 40 cm high: Stoelting Co., Wood Dale, IL) with a camera mounted above attached to a computer with Any-maze software to track movement (Stoelting Co.) as described⁵. On PID67 each rat was habituated to the empty AnyBox for 10 min. On PID68 rats were placed in the test arena with four identical objects, one in each corner. Exploration of objects was scored when rats were within 1 cm of an object. Rats had to accumulate 30 s of object exploration during the 10 min familiarization phase to be tested for retention 5 min later³³. For the retention phase, 3 copies of the familiarization objects and 1 novel object were placed in the corners of the AnyBox. Rats were again required to obtain 30 s of cumulative object exploration within 10 min. During familiarization and retention, most rats obtained 30 s of cumulative exploration in under 2 min. The dependent variable was novel object exploration time. Chance performance was 7.5 s.

Object in place

On PID74 rats were tested for object in place¹². The apparatus and procedures were the same as NOR with the following exceptions. During the familiarization phase there were 4 different objects, rather than identical

objects, one in each corner as before. The retention phase began 5 min after familiarization. For the retention phase, all objects were replaced with a copy and additionally two of the object positions were switched. During familiarization and retention, most rats obtained 30 s of cumulative exploration in 2–3 min. The dependent variable was novel position exploration time. Chance performance was 15 s.

Temporal order

On PID81–82 rats were tested for TO (Montay-Gruel et al., 2019). The apparatus and procedures were similar to NOR with the following exceptions. On PID81, rats were placed in the arena with only 2 identical objects until 30 s of exploration was reached (familiarization-1). One hour later, rats were placed back in the chamber with two different identical objects. Rats were tested until 30 s of object exploration occurred. On PID82, the test day, rats were placed in the arena with a copy of one object from familiarization-1 and one object from familiarization-2. Rats were removed from the arena after 30 s of cumulative object exploration. The dependent variable was exploration time of the object from familiarization-1. Chance performance was 15 s.

Straight channel

On PID83 rats were tested for straight channel swimming. The channel was 244 cm long \times 15 cm wide \times 50 cm deep and filled halfway with water ($21 \pm 1^\circ\text{C}$) with a submerged ($\sim 1\text{--}2$ cm) escape platform at one end as described⁵. Rats received 4 consecutive trials with a trial limit of 2 min. Each trial started with the rat placed in the water facing the wall opposite the escape platform. The straight channel swim teaches rats that escape from water is possible and is required for successful CWM performance. The dependent measure was latency to reach the platform.

Radial water maze

From PID84–PID85, rats were tested in the RWM as described with modification⁴⁴. The maze was a 210 cm diameter black polyethylene tank with 8 arms that were 55 cm long and 17 cm wide and filled halfway with water ($21 \pm 1^\circ\text{C}$). Posters were mounted on the walls. On the first trial of each day, all arms had submerged platforms at the end of the arms. Rats were started in the center and had 7 trials/day (limit 2 min/trial to locate a platform). Rats were removed after finding a platform and placed in a cage for 30 s. The found platform was removed and the next trial started. An entry into an arm without a platform was an error. Errors were defined as when the head and forelimbs crossed an imaginary line at the entrance of an arm. The average latency to find a platform on all trials was < 14 s. The dependent measures were latency to the platform and errors.

Morris water maze-acquisition and reversal

From PID86–PID99 rats were tested in the MWM acquisition and reversal phases^{45–47}. The pool was black and 244 cm in diameter, 51 cm deep, and filled half-way with water ($21 \pm 1^\circ\text{C}$). A black platform was submerged 2 cm below the surface in one quadrant depending on the test phase. Posters and geometric shapes were on the walls around the maze. There were 4 platform trials/day (max 2 min/trial) for 6 days and then a single probe trial (45 s with no platform) on the seventh day. Rats were run in rotation and the intertrial interval was 5 s spent on the platform plus the rotation time (3–10 min). For acquisition the platform was 10 cm diameter and located in the southwest quadrant (north was defined as the position furthest from the experimenter) and for reversal the platform was 7 cm diameter and located in the northeast quadrant. Rats were placed on the platform if they did not locate it within 2 min. For the learning trials, latency and path efficiency were analyzed. Path efficiency is independent of swim speed and is calculated as the length of a straight line from the start position to the platform divided by the length of path the rat took to reach the platform. For probe trials, the dependent measure was average distance from the former platform position⁴⁸.

Cincinnati water maze (CWM-A)

Rats were tested in the maze from PID100–PID123. The maze has 10 T-shaped cul-de-sacs branching from a 15 cm wide channel that extends from the start to the goal⁴⁹. The maze is 51 cm tall and filled halfway with water ($21 \pm 1^\circ\text{C}$). To preclude spatial navigation, and ensure only egocentric navigation was used, rats were run under infrared light. Rats were acclimated to the dark for at least 5 min prior to testing and given 2 trials/day with a 5 min limit/trial for 24 days. Experimenters scored latency to escape and errors with the use of an infrared sensitive camera mounted above the maze connected to a monitor in an adjacent room. If a rat did not find the goal, it was removed from the maze after 5 min and not guided to the escape platform. The second trial started after at least a 5 min rest period for rats that did not find the goal on trial-1 but started immediately after trial-1 for rats that found the goal. An error was counted similarly to the RWM at the stem of any dead-end cul-de-sac or at the crossing-arm of a “T”. An error correction for trials that reached the 5 min limit was the number of errors from the rat with the most errors, since some rats that could not find the escape on early trials treaded water and made few errors with maximum latency scores of 5 min. The dependent variables were latency and errors.

Morris water maze-shift, shift reversal, and cued-random

From PID138–PID153 rats were tested in the MWM in two additional phases (shift, shift reversal) followed by cued trials to assess proximal cue learning. All maze and room parameters were the same as above except that for shift and shift reversal the platform was 5 cm diameter. For the shift phase, the platform was in the northwest quadrant and for the shift reversal phase in the southeast quadrant. Dependent measures for the learning phase and probe phase were the same as above. The cued phase had 4 trials/day (2 min limit/trial) for 2 days, with a submerged 10 cm platform marked with a ball on a rod that protruded 10 cm above the water. Black curtains were closed around the pool to block distal cues. The platform and start positions were moved on each trial

rendering distal cues uninformative⁴⁵. The dependent measure for cued trials was latency since video tracking was not feasible with the lower lighting caused by the curtain around the maze.

Cincinnati water maze (CWM-B)

Next, rats were tested for 10 days from PID154–PID163 in the mirror image version. All parameters were the same as for CWM-A.

Novel object recognition

On PID164 NOR was tested in the same arena and same procedures, but without a day of habituation. During familiarization and retention, the average time to reach 30 s of cumulative exploration was < 200 s. The dependent variable was novel object preference time. Chance was 7.5 s.

ELISA assessment

On PID170, randomly selected rats ($n = 10/\text{group}$) were decapitated, and their brains were dissected over ice with the use of a brain block. The hippocampus and neostriatum were removed⁵⁰. Sections were rapidly frozen and stored at -80°C prior to analysis. ELISAs for AMPA-1, NMDA-R1, NMDA-R2, DRD-1, and TH were run per the manufacturer's instructions (MyBioSource, San Diego, CA). The limit of detection was 0.1 ng/mL for AMPA-1, 1 pg/mL for NMDA-R1, 0.1 ng/mL for NMDA-R2, 0.55 ng/mL for DRD-1, and 0.1 ng/mL for TH.

Experiment two: cytokine assessment

Cytokines in the hippocampus and neostriatum were assayed using the Meso Scale Discovery (MSD) proinflammatory panel-2 for rats V-PLEX® kit (MSD, Rockville, MD)²⁷. The cytokines on this panel were: interferon gamma (IFN- γ), interleukin 10 (IL-10), interleukin 13 (IL-13), IL-1 β , interleukin 4 (IL-4), interleukin 5 (IL-5), interleukin 6 (IL-6), keratinocyte chemoattractant/human growth-regulated oncogene (KC/GRO or CXCL1), and TNF- α . On PID2 or PID7, rats were decapitated, and their brains processed as above, frozen and stored at -80°C . All procedures were followed according to the manufacturer's protocol. The plate was analyzed by an MSD Meso Sector S600 plate reader, and concentrations were determined using MSD Discovery Workbench software®. Cytokine concentrations (pg/mL) were normalized to total protein (Protein Assay Kit (Pierce Biotechnology, Rockford, IL)) of each sample prior to analyses.

Statistical procedures

Data were analyzed using generalized linear mixed-effect models (SAS Proc Mixed, SAS Institute 9.4 TS, Cary, NC)⁵¹. Main effects of the irradiated groups versus Shams were first tested by one-sided Dunnett's tests since the effects of interest were adverse effects of proton exposure. Another Dunnett's test was used to compare all groups with the CV group. Other effects where no a priori predictions were made were tested using generalized linear mixed-effect models. Significant interactions were analyzed using the slice option in Proc Mixed since it controls the overall error term in the analyses. When irradiation was a factor for a significant interaction, Dunnett's test was used to sort the source of the effect. Repeated measure factors were fit to autoregressive moving average, autoregressive, or unstructured covariance⁵² depending upon best fit of the corrected Akaike Information Criterion. Repeated measures were week (body weights and locomotion), day (RWM, CWM-A, MWM, and CWM-B), block (ASR/TSR), trial type (ASR/TSR with acoustic or light prepulse), trial (straight water channel), or brain region (cytokines). The estimation method for the covariance parameters was by the restricted maximum likelihood method. Kenward-Roger first order adjusted degrees of freedom were used; these can be fractional, and were calculated for Type III ANOVAs⁵³. For survival data, a log-rank Mantel-Cox test was used in Graphpad Prism (version 9.3.1). Significance was set at $p \leq 0.05$. Data are presented as least square mean \pm SEM. Data were excluded for any rat that died during behavioral testing.

Data availability

Data are available at: Williams, Michael; Regan, Samantha; Fritz, Adam; Gollaway, Brooke; Mascia, Anthony; Vatner, Ralph; Perentesis, John; Vorhees, Charles (2024), "Data set for 18 Gy proton at different rates in Sprague Dawley rats", Mendeley Data, V1, doi: <https://doi.org/10.17632/xfjmxnfhct.1>.

Received: 21 June 2024; Accepted: 14 March 2025

Published online: 27 March 2025

References

1. Abayomi, O. K. Pathogenesis of irradiation-induced cognitive dysfunction. *Acta Oncol.* **35**(6), 659–663 (1996).
2. Son, Y. et al. Hippocampal dysfunctions caused by cranial irradiation: A review of the experimental evidence. *Brain Behav. Immun.* **45**, 287–296 (2015).
3. Kahalley, L. S. et al. Superior intellectual outcomes after proton radiotherapy compared with photon radiotherapy for pediatric medulloblastoma. *J. Clin. Oncol.* **38**(5), 454–461 (2020).
4. Tang, T. T. et al. Cognitive and imaging differences after proton and photon whole brain irradiation in a preclinical model. *Int. J. Radiat. Oncol. Biol. Phys.* **112**(2), 554–564 (2022).
5. Williams, M. T. et al. Whole brain proton irradiation in adult Sprague Dawley rats produces dose dependent and non-dependent cognitive, behavioral, and dopaminergic effects. *Sci. Rep.* **10**(1), 21584 (2020).
6. Friedl, A. A. et al. Radiobiology of the FLASH effect. *Med. Phys.* **49**(3), 1993–2013 (2022).
7. Gao, Y. et al. A potential revolution in cancer treatment: A topical review of FLASH radiotherapy. *J. Appl. Clin. Med. Phys.* **23**(10), e13790 (2022).
8. Cunningham, S. et al. FLASH proton pencil beam scanning irradiation minimizes radiation-induced leg contracture and skin toxicity in mice. *Cancers* **13**(5), 1012 (2021).

9. Mascia, A. E. et al. Proton FLASH radiotherapy for the treatment of symptomatic bone metastases: The FAST-01 nonrandomized trial. *JAMA Oncol.* **9**(1), 62–69 (2023).
10. Alagband, Y. et al. Uncovering the protective neurologic mechanisms of hypofractionated FLASH radiotherapy. *Cancer Res. Commun.* **3**(4), 725–737 (2023).
11. Alagband, Y. et al. Neuroprotection of radiosensitive juvenile mice by ultra-high dose rate FLASH irradiation. *Cancers* **12**(6), 1671 (2020).
12. Montay-Gruel, P. et al. Long-term neurocognitive benefits of FLASH radiotherapy driven by reduced reactive oxygen species. *Proc. Natl. Acad. Sci. U. S. A.* **116**(22), 10943–10951 (2019).
13. Pawelke, J. et al. Electron dose rate and oxygen depletion protect zebrafish embryos from radiation damage. *Radiother. Oncol.* **158**, 7–12 (2021).
14. Vozenin, M.-C. et al. The advantage of FLASH radiotherapy confirmed in mini-pig and cat-cancer patients. *Clin. Cancer Res.* **25**(1), 35–42 (2019).
15. Montay-Gruel, P. et al. Irradiation in a flash: Unique sparing of memory in mice after whole brain irradiation with dose rates above 100Gy/s. *Radiother. Oncol.* **124**(3), 365–369 (2017).
16. Montay-Gruel, P. et al. Hypofractionated FLASH-RT as an effective treatment against glioblastoma that reduces neurocognitive side effects in mice. *Clin. Cancer Res.* **27**(3), 775–784 (2021).
17. Allen, B. D. et al. Elucidating the neurological mechanism of the FLASH effect in juvenile mice exposed to hypofractionated radiotherapy. *Neuro Oncol.* **25**, 927–939 (2022).
18. Shukla, S. et al. Ultra-high dose-rate proton FLASH improves tumor control. *Radiother. Oncol.* **186**, 109741 (2023).
19. Williams, M. T. et al. Cognitive and behavioral effects of whole brain conventional or high dose rate (FLASH) proton irradiation in a neonatal Sprague Dawley rat model. *PLOS ONE* **17**(9), e0274007 (2022).
20. Iturri, L. et al. Proton FLASH radiation therapy and immune infiltration: Evaluation in an orthotopic glioma rat model. *Int. J. Radiat. Oncol. Biol. Phys.* **116**(3), 655–665 (2023).
21. Zhang, Q. et al. FLASH investigations using protons: Design of delivery system, preclinical setup and confirmation of FLASH effect with protons in animal systems. *Radiat. Res.* **194**(6), 656–664 (2020).
22. Zhang, Q. et al. Proton FLASH effects on mouse skin at different oxygen tensions. *Phys. Med. Biol.* **68**(5), 055010 (2023).
23. Sørensen, B. S. et al. Pencil beam scanning proton FLASH maintains tumor control while normal tissue damage is reduced in a mouse model. *Radiother. Oncol.* **175**, 178–184 (2022).
24. Silverman, J. L. et al. Reconsidering animal models used to study autism spectrum disorder: Current state and optimizing future. *Genes Brain Behav.* **21**(5), e12803 (2022).
25. Cnops, V. et al. Test, rinse, repeat: A review of carryover effects in rodent behavioral assays. *Neurosci. Biobehav. Rev.* **135**, 104560 (2022).
26. Vorhees, C. V. & Williams, M. T. Issues in the design, analysis, and application of rodent developmental neurotoxicology studies. *Neurotoxicol. Teratol.* **87**, 107018 (2021).
27. Simmons, D. A. et al. Reduced cognitive deficits after FLASH irradiation of whole mouse brain are associated with less hippocampal dendritic spine loss and neuroinflammation. *Radiother. Oncol.* **139**, 4–10 (2019).
28. Zheng, A. & Schmid, S. A review of the neural basis underlying the acoustic startle response with a focus on recent developments in mammals. *Neurosci. Biobehav. Rev.* **148**, 105129 (2023).
29. Parham, K. & Willott, J. F. Effects of inferior colliculus lesions on the acoustic startle response. *Behav. Neurosci.* **104**(6), 831–840 (1990).
30. Li, L. et al. Prepulse inhibition following lesions of the inferior colliculus: Prepulse intensity functions. *Physiol. Behav.* **65**(1), 133–139 (1998).
31. Morris, R. G. et al. Ibotenate lesions of hippocampus and/or subiculum: Dissociating components of allocentric spatial learning. *Eur. J. Neurosci.* **2**(12), 1016–1028 (1990).
32. Morris, R. G. M. et al. Place navigation impaired in rats with hippocampal lesions. *Nature* **297**, 681–683 (1982).
33. Clark, R. E., Zola, S. M. & Squire, L. R. Impaired recognition memory in rats after damage to the hippocampus. *J. Neurosci.* **20**(23), 8853–8860 (2000).
34. Braun, A. A. et al. Dopamine depletion in either the dorsomedial or dorsolateral striatum impairs egocentric Cinnati water maze performance while sparing allocentric Morris water maze learning. *Neurobiol. Learn. Mem.* **118**, 55–63 (2015).
35. Braun, A. A. et al. Dorsal striatal dopamine depletion impairs both allocentric and egocentric navigation in rats. *Neurobiol. Learn. Mem.* **97**(4), 402–408 (2012).
36. Braun, A. A. et al. 6-Hydroxydopamine-Induced dopamine reductions in the nucleus accumbens, but not the medial prefrontal cortex, impair Cinnati water maze egocentric and Morris water maze allocentric navigation in male Sprague-Dawley rats. *Neurotox. Res.* **30**(199), 212 (2016).
37. Hinman, J. R., Chapman, G. W. & Hasselmo, M. E. Neuronal representation of environmental boundaries in egocentric coordinates. *Nat. Commun.* **10**(1), 2772 (2019).
38. Vorhees, C. V. et al. Effects of neonatal (+)-methamphetamine on path integration and spatial learning in rats: Effects of dose and rearing conditions. *Int. J. Dev. Neurosci.* **26**(6), 599–610 (2008).
39. Lourenço, A. et al. Absolute dosimetry for FLASH proton pencil beam scanning radiotherapy. *Sci. Rep.* **13**(1), 2054 (2023).
40. Folkerts, M. M. et al. A framework for defining FLASH dose rate for pencil beam scanning. *Med. Phys.* **47**(12), 6396–6404 (2020).
41. Regan, S. L. et al. Knockout of latrophilin-3 in Sprague-Dawley rats causes hyperactivity, hyper-reactivity, under-response to amphetamine, and disrupted dopamine markers. *Neurobiol. Dis.* **130**, 104494–104494 (2019).
42. Pitzer, E. M. et al. Deltamethrin exposure daily from postnatal day 3–20 in Sprague-Dawley rats causes long-term cognitive and behavioral deficits. *Toxicol. Sci.* **169**(2), 511–523 (2019).
43. Regan, S. L. et al. Effects of permethrin or deltamethrin exposure in adult Sprague Dawley rats on acoustic and light prepulse inhibition of acoustic or tactile startle. *Neurotox. Res.* **39**, 543–555 (2021).
44. Yermakov, L. M. et al. Impairment of cognitive flexibility in type 2 diabetic db/db mice. *Behav. Brain Res.* **371**, 111978 (2019).
45. Vorhees, C. V. & Williams, M. T. Morris water maze: Procedures for assessing spatial and related forms of learning and memory. *Nat. Protoc.* **1**(2), 848–858 (2006).
46. Vorhees, C. V. & Williams, M. T. Assessing spatial learning and memory in rodents. *ILAR J.* **55**(2), 310–332 (2014).
47. Vorhees, C. V. & Williams, M. T. Value of water mazes for assessing spatial and egocentric learning and memory in rodent basic research and regulatory studies. *Neurotoxicol. Teratol.* **45**, 75–90 (2014).
48. Maei, H. et al. What is the most sensitive measure of water maze probe test performance?. *Front. Integr. Neurosci.* **3**(4), 493 (2009).
49. Vorhees, C. V. & Williams, M. T. Cinnati water maze: A review of the development, methods, and evidence as a test of egocentric learning and memory. *Neurotoxicol. Teratol.* **57**, 1–19 (2016).
50. Williams, M. T. et al. Alterations in body temperature, corticosterone, and behavior following the administration of 5-methoxy-diisopropyltryptamine ('foxy') to adult rats: A new drug of abuse. *Neuropsychopharmacology* **32**(6), 1404–1420 (2007).
51. Yu, Z. et al. Beyond t test and ANOVA: Applications of mixed-effects models for more rigorous statistical analysis in neuroscience research. *Neuron* **110**(1), 21–23 (2022).
52. Wolfinger, R. Covariance structure selection in general mixed models. *Commun. Stat. Simul. Comput.* **22**(4), 1079–1106 (1993).
53. McNeish, D. Small sample methods for multilevel modeling: A colloquial elucidation of REML and the Kenward-Roger correction. *Multivariate Behav. Res.* **52**(5), 661–670 (2017).

Author contributions

M.T.W.—Conceptualization, Formal Analysis, Funding Acquisition, Project Administration, Supervision, Visualization, Writing—Original Draft Preparation, Writing—Review & Editing S.L.R.—Investigation, Writing—Review & Editing A.L.F.—Data Curation, Investigation, Writing—Review & Editing B.M.G.—Data Curation, Investigation, Writing—Review & Editing A.E.M.—Resources, Writing—Review & Editing R.E.V.—Conceptualization, Writing—Review & Editing J.P.P.—Conceptualization, Funding Acquisition, Writing—Review & Editing C.V.V.—Conceptualization, Funding Acquisition, Project Administration, Supervision, Visualization, Writing—Original Draft Preparation, Writing—Review & Editing.

Funding

This research was supported by a Research Agreement with Varian Medical Systems, a Siemens Healthineers Company. Additional funding included research support from the TQL Foundation, Cincinnati, OH, Fund the Cure Next Door Foundation, and NIH P30 ES006096.

Declarations

Competing interests

Drs. Williams, Mascia, Vatner, Perentesis, and Vorhees received funding from Varian Medical Systems, Inc. Dr. Regan, Dr. Pitzer, Mr. Fritz, and Ms. Gollaway have no competing interests. No author has any non-financial competing interests. Experiments were funded by Varian Medical Systems that granted authors intellectual freedom to publish the data without restriction.

Additional information

Correspondence and requests for materials should be addressed to M.T.W.

Reprints and permissions information is available at www.nature.com/reprints.

Publisher's note Springer Nature remains neutral with regard to jurisdictional claims in published maps and institutional affiliations.

Open Access This article is licensed under a Creative Commons Attribution-NonCommercial-NoDerivatives 4.0 International License, which permits any non-commercial use, sharing, distribution and reproduction in any medium or format, as long as you give appropriate credit to the original author(s) and the source, provide a link to the Creative Commons licence, and indicate if you modified the licensed material. You do not have permission under this licence to share adapted material derived from this article or parts of it. The images or other third party material in this article are included in the article's Creative Commons licence, unless indicated otherwise in a credit line to the material. If material is not included in the article's Creative Commons licence and your intended use is not permitted by statutory regulation or exceeds the permitted use, you will need to obtain permission directly from the copyright holder. To view a copy of this licence, visit <http://creativecommons.org/licenses/by-nc-nd/4.0/>.

© The Author(s) 2025